2015-01-01

Alternative Fatigue Cracking Resistance Assessment Criteria Of Asphalt Mixtures With Overlay Tester

Alejandro Miramontes
University of Texas at El Paso, amiramontes4@miners.utep.edu

ALTERNATIVE FATIGUE CRACKING RESISTANCE ASSESSMENT CRITERIA OF ASPHALT MIXTURES WITH OVERLAY TESTER

ALEJANDRO MIRAMONTES

Department of Civil Engineering

APPROVED:

Soheil Nazarian, Ph.D., co-Chair

Imad Abdallah, Ph.D., co-Chair

Calvin Stewart, Ph.D.

Charles Ambler, Ph.D.
Dean of the Graduate School

Dedication

I would like to dedicate this thesis to my parents, my brother and sister.

ALTERNATIVE FATIGUE CRACKING RESISTANCE ASSESSMENT CRITERIA OF ASPHALT MIXTURES WITH OVERLAY TESTER

by

ALEJANDRO MIRAMONTES, BSCE

THESIS

Presented to the Faculty of the Graduate School of

The University of Texas at El Paso

in Partial Fulfillment

of the Requirements

for the Degree of

MASTER OF SCIENCE

Department of Civil Engineering

THE UNIVERSITY OF TEXAS AT EL PASO

December 2015

Acknowledgements

I would like to express my sincere appreciation to my thesis and project advisor, Dr. Soheil Nazarian for providing me the opportunity to work at the Center for Transportation Infrastructure Systems. His guidance, suggestions and supervision were fundamental for this project and definitely for this thesis. It has been an outstanding experience working with him. I would also like to thank and express my gratefulness to Dr. Imad Abdallah, who helped me to develop most of my analytical skills, without his faith in me and advice this would not have been possible. It is a pleasure to say that I worked under his supervision as well. Finally, I would like to thank my co-worker Victor Garcia who has helped me in vast aspects of my research and has been a key piece during the development of this project. His commitment to the Center and to this project is something to admire. To the laboratory manager, Mr. Jose Garibay, I would like to express my gratitude for providing me with the help I needed.

During the development of this project and thesis I had the opportunity to collaborate with other professionals. I would like to extend my gratitude to Dr. Robert Lee and Mrs. Gisel Carrasco. Also, I would like to thank all my committee members including Dr. Calvin Stewart, for taking the time to review this thesis.

I am very grateful to Dr. Anjan Kumar Siddagangaiah, a person and friend who helped me in my beginnings at the Center with his expertise in pavement design. I also want to thank my friends Heber Prieto, Jorge Alvarez, Manuel Gutierrez, Ramon Cardona and Jorge Beltran for their unconditional support, great experiences and advice during those times I needed them the most.

Finally, I would like to thank and dedicate this thesis to my family: my father, Jesus Miramontes, my mother, Rosario Miranda, my brother, Jesus A. Miramontes, and my sister, Fabiola Miramontes, for the uninterrupted support and motivation to obtain everything.

Abstract

The accumulation of damage due to cracking of hot mix asphalt (HMA) layers under repeated loading along with the climatic effects is known as fatigue cracking. The Overlay Tester (OT) has been implemented or considered by several highway agencies as an index to evaluate the cracking susceptibility and resistance to cracking of asphalt mixtures in the laboratory. The performance indicator used to measure the quality of the HMA mixes is the number of cycles that a specimen may resist during the test until the crack appears and fully propagates to the top of the specimen. The repeatability of the number of cycles to failure measured with the OT is expressed as a concern to reliably assess the potential of asphalt mixtures to cracking.

The goal of this thesis is to methodically evaluate the performance of the current OT test protocol. By addressing alternative cracking test methods and parameters a surrogate performance indicator may reliably estimate the fatigue cracking properties of HMA mixes. Fundamentally, cracking can be characterized in two stages: a) crack initiation and b) crack propagation. In this study, the focus was to analyze the data from the OT test considering these two stages. An alternative failure criteria to rank and screen the cracking resistance of asphalt mixtures was developed for the current OT test

Table of Contents

List of Tables

List of Figures

List of Illustrations

Chapter 1: Introduction

Presently, the accumulation of damage due to cracking of HMA layers is a major concern observed on flexible pavements, which deteriorates the pavement structures at a rapid rate. A hot mix asphalt (HMA) layer must have a balance of both good rut and crack resistance properties to perform well in the field (Germann and Lytton, 1979; Zhou et al., 2006). Over the past decade, HMA mixes have been modified to improve their rutting potential using wheel-tracking tests such as the Hamburg tests. Stiffer binders and good stone-to-stone contact may improve rut resistance but they may also reduce the mix flexibility and cracking resistance of the HMA (Zhou and Scullion, 2006).

Cracking occurs due to the tensile stresses imposed by traffic loads exceeding the tensile strength of asphalt layers. The moisture damage and climatic effects also significantly influence the performance of the HMA layers in the field. Premature cracking on HMA layers continues to be a recurring problem for the pavement community especially with the aging of the asphalt layer in existing pavements and the intricacy of the new mix designs utilizing more additives and recycled materials. A testing procedure and thorough specifications are required at the level of mixture selection and design to ensure the desired performance of asphalt pavements against cracking.

Several highway agencies have either implemented or considered implementing performance tests to estimate the cracking resistance of HMA mixes in the laboratory setting. A number of test methods like the traditional indirect tensile (IDT) test, the semi-circular bending (SCB) test or the disk-shape compact tension (DCT) test are some examples of available tests to evaluate the cracking characteristics of the HMA mixes. One such popular test, the overlay tester

(OT), measures the number of cycles to failure of HMA specimens by simulating the opening and closing of joints and/or cracks induced by daily temperature variations and high tensile strain generated by traffic load. However, the repeatability in the results is reported as the main challenge for employing OT to evaluate the cracking resistance of HMA mixes. The use of OT to measure resistance to cracking of HMA reliably and in a robust manner is greatly needed for all mixture types and HMA specifications.

Recently, a great deal of effort has been directed toward the improvement of testing and analysis methods to study the cracking mechanism of asphalt pavements using OT (Jacobs et al., 1996; Medani et al., 2000; Marasteanu et al., 2002; Wagoner et al., 2005; Hajj et al., 2010). For this thesis, a rigorous evaluation of OT data from a dense-graded HMA mix was carried out to outline surrogate approaches for assessing the cracking resistance of asphalt mixtures. Alternative data interpretation methods were investigated to improve the repeatability of OT results. Also, a promising approach that can predict the cracking resistance with less variation in the results was delineated from a rigorous evaluation. The alternative approach was investigated using several HMA mixes to examine its applicability and effectiveness on all types of asphalt mixtures. This thesis was carried out as part of the research project 0-6815, sponsored by the Texas Department of Transportation (TxDOT), "Improved Overlay Tester Procedure for Fatigue Cracking Resistance of Asphalt Mixtures". This thesis detailed the process of investigating alternative data interpretation methods, the performance of promising approaches, and the application of new approaches to estimate and rank the cracking resistance of HMA mixes.

1.1 LITERATURE REVIEW

Premature cracking is a predominant type of distress observed in the pavement structure due to vehicular loads and climatic effects. Agencies in the US and worldwide have implemented testing procedures and empirical relationships to predict the cracking properties of HMA from conventional material parameters, such as tensile strength and modulus (Wagoner et al., 2005). At present, no single laboratory test has been established as the widely accepted standard cracking test that can be performed routinely during the laboratory mixture design process to ensure that HMA is not susceptible to premature cracking.

The OT was first introduced by Germann and Lytton (1979) to predict the reflective cracking resistance of asphalt overlays on long beam specimens. Zhou and Scullion (2003) proposed to modify the specimen's dimensions for the use of both laboratory prepared and field cores. The results from the modified test setup were validated with field observations. Zhou et al. (2005) evaluated two alternatives for determining the cracking resistance in terms of number of cycles to failure. First approach was based on the change in the response of material to constant displacement (called "loading shape method"). The other alternative was based on the reduction in the maximum load.

In the loading shape method, three distinct phases were observed: (I) crack initiation and steady propagation, (II) late crack propagation, and (III) failure (see Figure 1.1). Several traditional cracking models have been used to explain the crack growth mechanism in asphalt layers (Ghuzlan and Carpenter, 2003). Linear fracture mechanics and continuum damage mechanics frameworks have been explored to characterize the crack growth mechanisms (Zhang et al., 2001; Roque et al., 2002; Zhou et al., 2009; Jacobs et al., 1995; Koohi et al., 2012). The

crack initiation and propagation depend on the material, geometry and load levels. At low load/displacement levels, the energy is expended in nucleating cracks rather than propagating them. At high load/displacement levels, plastic deformation takes place rapidly leading to failure (Pungo et al., 2006). Based on this philosophy, Zhou et al. (2005) recommended a 0.025 in. displacement in the OT for evaluating the cracking resistance of asphalt mixtures

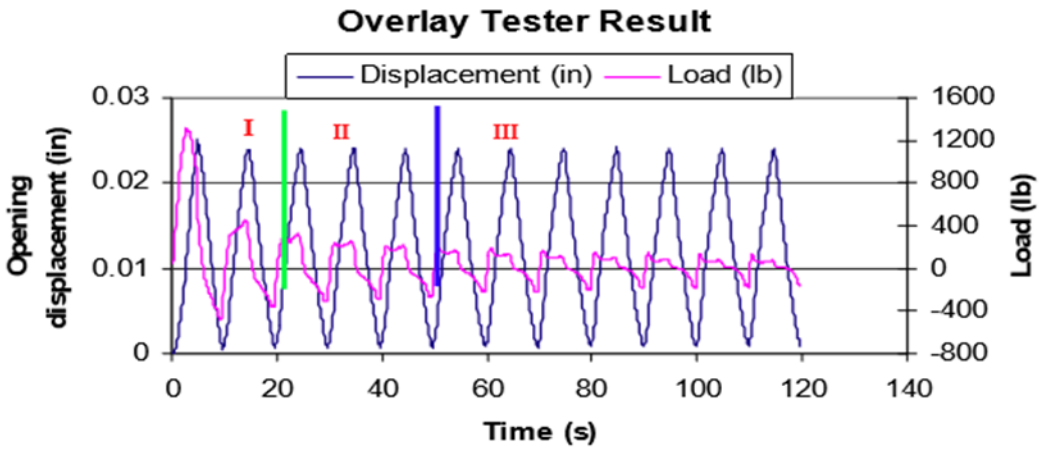

Figure 1.1: Typical OT Output Data (Zhou et al. 2005)

For the reduction in the maximum load method, the number of cycles was established as the failure criteria. The number of cycles was obtained at the 93% reduction in load from the maximum load of the first cycle. This criteria was proposed based on the performance of 200 specimens from different HMA mixes. It was concluded that asphalt mixtures failing after 300 load cycles at 93% load reduction were resistant to cracking. Zhou et al. (2005) also showed that the influence of air void content was not significant on cracking resistance. Zhou et al. (2007) recommended using the OT test in conjunction with the Hamburg rutting test to design asphalt mixes with adequate reliability against rutting and cracking resistance.

Additionally, Zhou et al. (2009) modified the OT to measure the fatigue cracking resistance of asphalt mixes based on the principles of fracture mechanics. A backcalculation method was proposed to estimate the crack length and fracture parameters A and n. Later, Hu et al. (2012) presented the required modifications for the present OT to measure the cracking properties. The enhancement was incorporated to characterize the Mode I (bending or tensile mode) type of fracture in the asphalt mixtures due to repeated loads and to measure the modulus of asphalt mixtures under tension mode. The backcalculated crack length depends on the calibration with actual measurements using digital image correlation (DIC) technique, which might increase the variability in the estimated parameters due to different type of mixtures, binder type and volumetric properties.

Zhou and Scullion (2003) performed a sensitivity study to analyze the influence of operational parameters such as test temperature, opening displacement, air voids, asphalt performance grade, and asphalt content, on the variability of the results. They found the OT results are sensitive to the key components of HMA mixtures such as the grade of asphalt binder, asphalt binder content, air voids, and aggregate properties. Walubita et al. (2012) studied comprehensively a number of parameters that influenced the repeatability of OT results, especially for coarse and dense-graded mixes. Walubita et al. (2012) noted that one of the key problems contributing to the reported high variability in the OT test results was primarily related to non-adherence to the specifications and OT test procedures. Walubita et al. (2012) also concluded that, aside from the HMA response behavior, the variability in the OT test might be a function of the sample fabrication and test setup. Recommendations were given for the gluing method, sample drying method, curing time prior to testing, and the sample conditioning time to reduce the variability on the results. Although those studies helped to improve the OT procedure, the variability of the number of cycles

measured with the OT test is still a concern to reliably determine the reflective cracking resistance of HMA specimens in the laboratory setting.

Walubita et al. (2013) proposed a monotonic testing protocol using overlay tester to screen and rank asphalt mixes similar to Fenix and indirect tensile test. Fracture energy and fracture energy index were identified as the parameters to distinguish the fracture resistance of asphalt mixes. Parametric sensitivity analysis was carried out in comparison with repeated load overlay testing to address the variability with different asphalt mix types (as shown in Figure 1.2). They concluded that fracture energy index could be used to rank the asphalt mixtures with low variability in comparison to standard OT procedure (as shown in Figure 1.3).

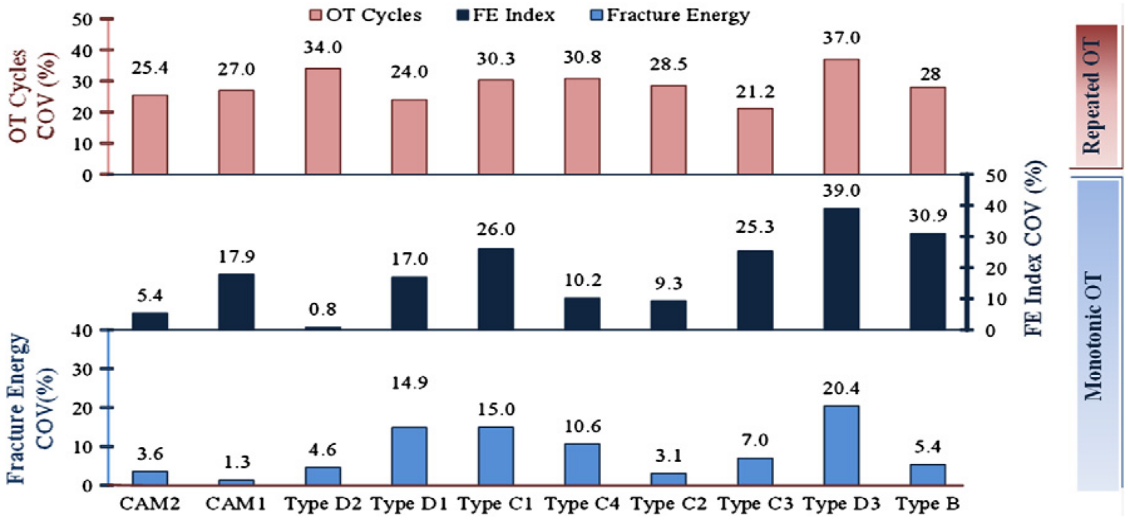

Figure 1.2: Variability in OT Results with Different Asphalt Mixtures (Walubita et al. 2013)

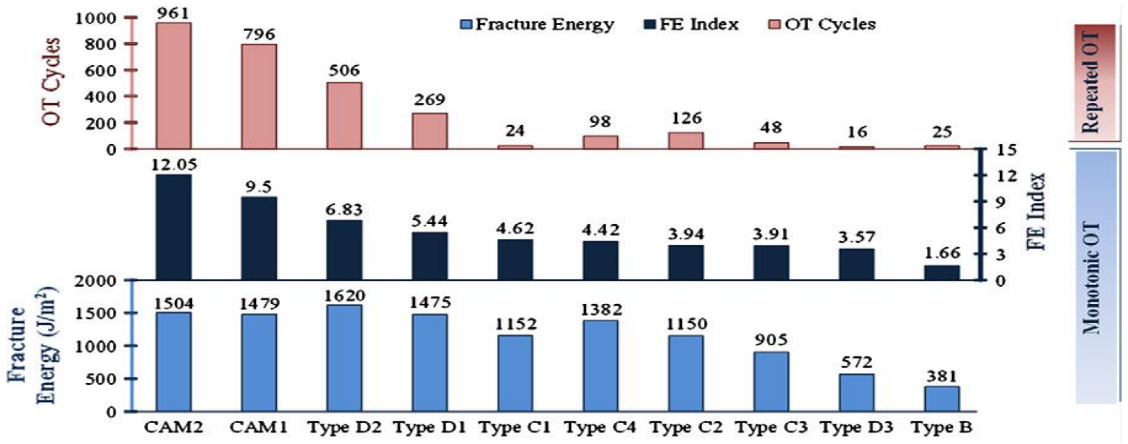

Figure 1.3: Ranking of Asphalt Mixtures Using Monotonic OT (Walubita et al. 2013)

In summary, there has been extensive effort and research to characterize crack initiation and crack propagation of HMA specimens using OT. The direct measurement of OT fracture parameters has become highly important to evaluate its potential to screen cracking resistance of asphalt mixtures. At present, no single laboratory test has been established as the widely accepted standard cracking test that can be performed routinely during the laboratory mixture design process to ensure that HMA is not susceptible to premature cracking. The development and evaluation of valid performance tests suitable for characterizing cracking potential of HMA mixes are considered indispensable steps to improve the performance of flexible pavements.

1.2 OVERLAY TESTER

Detailed information about the OT test procedure is outlined in the TxDOT test procedure Tex-248-F, which is similar to the ASTM WK26816 protocol. The test is conducted in a displacement-controlled mode at a repeated loading rate of one cycle per 10 sec. The sliding platen moves in a cyclic triangular waveform to a constant maximum displacement of 0.025 in. (635 µm) at a test temperature of 77ºF (25ºC). The primary output of the OT test is the number of cycles for the HMA specimen to lose 93% of its initial strength in the cracking mode.

Illustration 1.1 shows the key components of an OT specimen mounted onto the OT plates. The OT specimens are nominally 6 in. (150 mm) long, 3 in. (75 mm) wide and 1.5 in. (38 mm) thick. The specimens are trimmed from the standard 6 in. (150 mm) diameter by 4.5 in. (114 mm) thick bricketts compacted with a Superpave Gyratory Compactor (SGC) in accordance with the AASHTO T312 (ASTM D-6925) protocol to a nominal air-void target of 7±1.0%. The OT specimens can also be prepared from field cores or slabs. The OT specimens are glued to the two horizontal platens with half of the length of the specimen resting on each platen. The accumulation of the glue in the gap between the base plates (marked as "a" in Illustration 1.1) and the uniformity of the glued area (marked as "b") could be the potential sources of variability. As described by Garcia and Miramontes (2015), a linear variable differential transformer (LVDT) was added to the test setup (marked as "c") to ensure that the specimens do not experience significant bending since the OT load is applied eccentric to the neutral axis of the specimen.

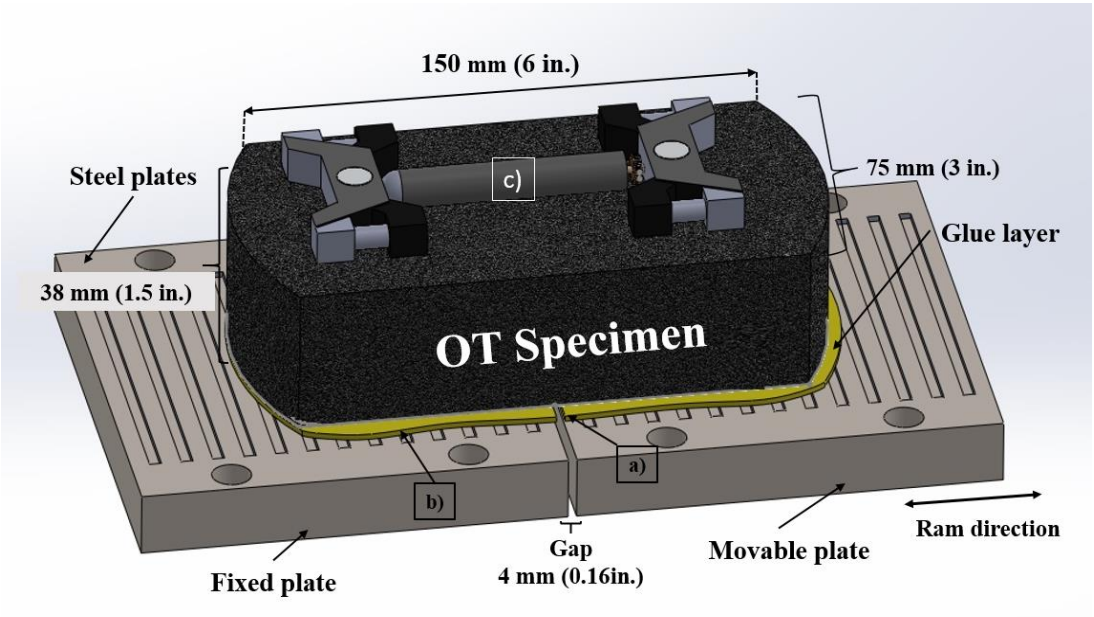

Illustration: 1.1 OT Schematic Layout and Sample Setup

During the overlay test, the device automatically records the time histories of the applied load, the actuator displacement, the top LVDT displacement (if installed), the number of load cycles, and the test temperature. Figure 1.4 shows the typical data obtained from the OT test. The displacement and load acquired for each cycle can be plotted against one another to inspect the hysteretic behavior (load-displacement curve) of the mix as shown in Figure 1.4b. The first cycle provides the maximum load where the initial damage (crack initiation phase) occurs. The remaining cycles represent the crack propagation phase until the failure limit of 93% of maximum load is reached.

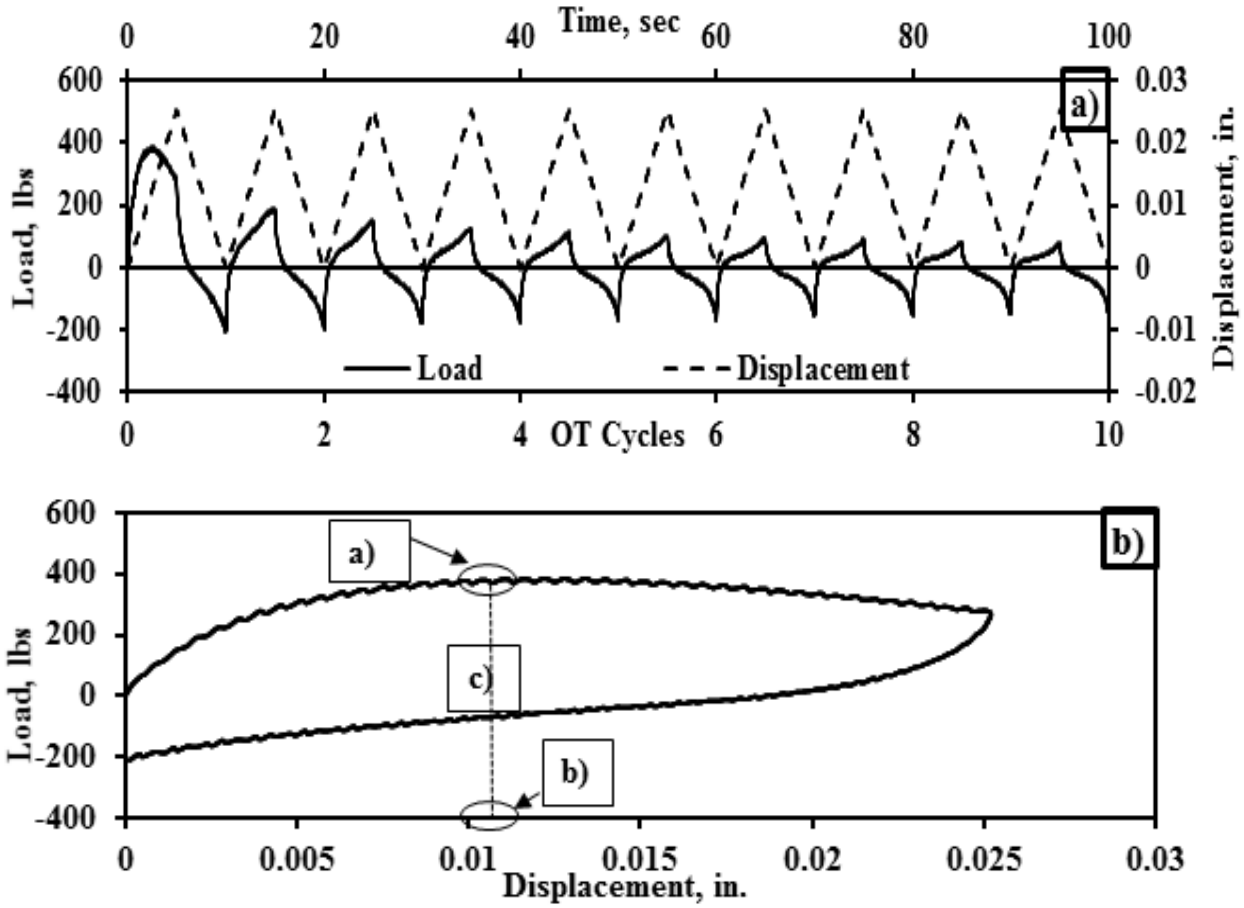

Figure 1.4: Interpretation of OT Results: Typical OT Data and b) Load-Displacement Response Curve (Hysteresis Loop)

Chapter 2: Current Overlay Tester Performance Index

The purpose of this chapter is to summarize previous work performed on the current OT performance index. This chapter describes a multi-laboratory study developed by UTEP in collaboration with TxDOT on assessing the variability of the OT test. It also covers changes implemented in the current experimental setup of the OT test and the inconsistencies of the current performance index.

2.1 PREVIOUS WORK

A study requested by TxDOT to determine the variability of the OT tests in a multi-laboratory environment on a large number of specimens from one HMA mix. The objective was to assess the variability of the OT test using several specimens of the same HMA mix. In collaboration with TxDOT, over sixty specimens were prepared from a dense-graded (Type-C) mix. All specimens were prepared, molded and trimmed by an experienced TxDOT personnel to maintain a consistent sample preparation and to minimize the variability related to the use of different operators and different laboratory equipment. Thirty-two specimens were tested at UTEP and thirty-two specimens at TxDOT central laboratory. The gap between the plates used on these OT tests was 4 mm as was implemented by TxDOT.

The summary of the results from this study is shown in Table 2.1. Three parameters were identified as critical in assessing the variability of the OT tests: (1) the maximum load, (2) the last load and (3) the number of cycles to failure. The averages and the standard deviations of the three parameters were consistent between the two laboratories. The maximum load and last load were repeatable with coefficients of variation (COV) of less than 10%. The COVs of the numbers of

cycles to failure were in excess of 73%. Based on the results of this activity, the focus of the study was shifted to the experimental setup.

Table 2.1: Summary of Multi-Laboratory Study

Agency	Statistical Parameter	Cycles to Failure	Maximum Load (lbs)	Last Load (lbs)
UTEP	Average	58	838	57
	Standard Deviation	49	63	4
	COV	83%	7%	8%
TxDOT	Average	57	908	56
	Standard Deviation	41	65	5
	COV	73%	7%	8%

2.2 EVALUATION OF EXPERIMENTAL SETUP

Walubita et al. (2012) noted that one of the problems contributing to the reported high variability in the OT test results might be related to non-adherence to the specifications and/or test procedures. They concluded that, aside from the HMA response behaviors, the variability in the OT test might be a function of the sample fabrication and test setup. During the previously mentioned ongoing research project 0-6815, several key variables associated with the Tex-248-F procedure were thoroughly investigated (the detailed study is shown in Appendix A). Two of the more critical set up parameters were found to be the gluing procedure and the glue type.

The gluing procedure was modified by incorporating petroleum jelly and tape in the middle of the trimmed specimens to ensure a consistent glued area. In addition, the excess glue that squeezed out during the curing with a sustained load on top of the specimen generated undesirable interaction between the specimen and the plate. The applied load was reduced from 10 lbs to 5 lbs to increase the thickness of the epoxy layer and thereby strengthening the bond as recommended by the glue manufacturer. The excess glue that squeezed out was also carefully removed when fresh to ensure a uniform bond only between the specimen and the bottom platen. These practical

issues along with a few others improved the repeatability of the test parameters as detailed in Appendix A.

The glue suggested in Tex-248-F OT protocol (2500-psi) was changed for a stronger glue (4400-psi) to minimize the interaction among the glue, HMA and the steel plates. As a result of this study, the hysteresis loops were more linear and repeatable with the stronger glue than the one suggested in the OT protocol.

The evaluation of the monotonic OT test, which consists of one unidirectional movement to cause the total failure of the specimen, was also reported in this study, as shown in Appendix A. The monotonic OT tests were conducted on the synthetic specimens up to a maximum opening displacement (MOD) of 0.125 in. The 4400-psi epoxy demonstrated to resist higher maximum loads before the synthetic specimen detached from the plates due to the monotonic OT mechanism, than the suggested 2500-psi epoxy.

Figure 2.1 shows the first-cycle hysteresis loops (load versus displacement curves) based on the modified experimental setup for five specimens of the same Type C mix used in Table 1. The hysteresis loops were repeatable as quantified in Table 2.2. The maximum load and the area inside the hysteresis loop showed the highest repeatability. While the repeatability of the number of cycles to failure improved based on the modified experimental setup, it was still deemed high.

The modified experimantal setup was evaluated with another set of Type C mix specimens under the monotonic OT tests. Figure 2.2 shows the superposition of the hysteresis loop curves of the Type C mix specimens subjected to monotonic OT. Table 2.3 summarizes the results obtained. The maximum loads were more repeatable than the displacements at the maximum load.

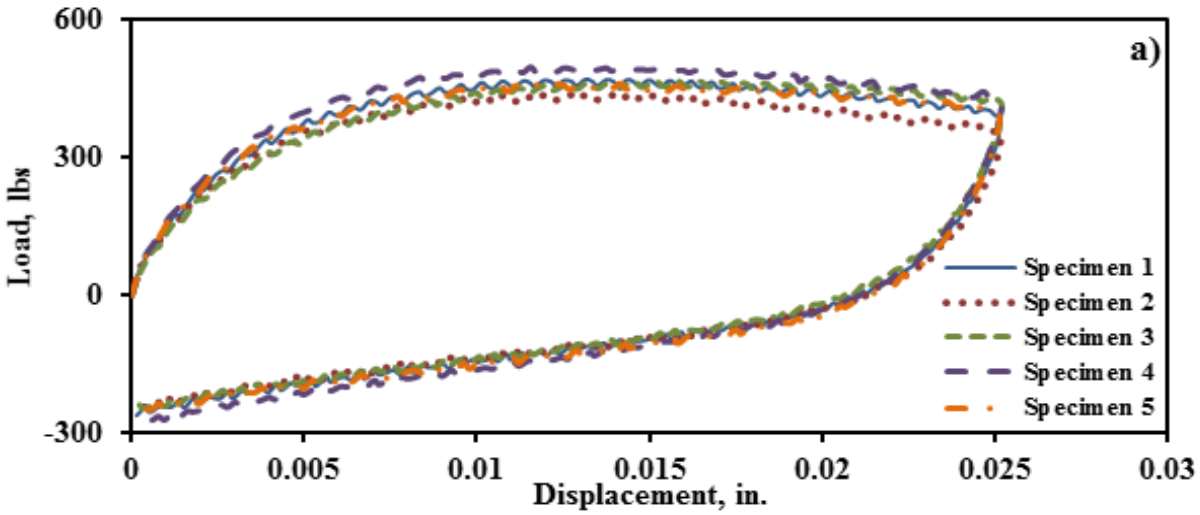

Figure 2.1: Repeatability of Hysteresis Loops after Gluing Process Modifications (Type C Mix)

Table 2.2: Summary of Results of Type C Mix (Cyclic OT)

Parameter	Number of OT Cycles	Maximum Load, lbs	Displacement at Maximum Load, in.	Area of Hysteresis Loop, lbs-in.
Average	300	467	0.014	12
Std. Dev.	95	21	0.002	1
COV	32%	4%	12%	5%

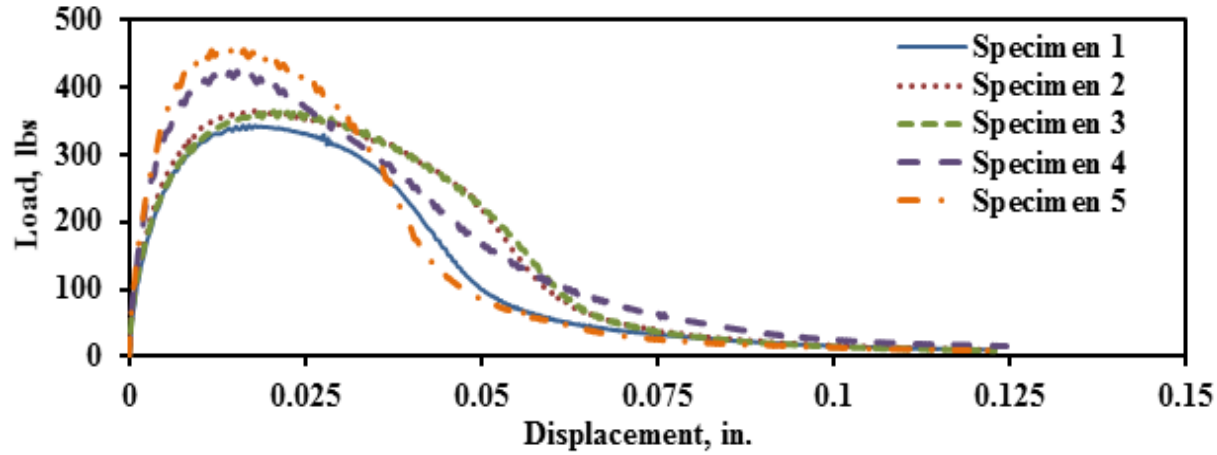

Figure 2.2: Hysteresis Loops of Type C Specimens under Monotonic OT

Table 2.3: Summary of Results of Type C Mix (Monotonic OT)

Parameters	Maximum Load, lbs	Displacement at Max Load, in.	Air Voids %
Average	391	0.017	6.9
Std. Dev.	47	0.003	0.4
COV	12%	16%	6%

In conclusion, the new experimental procedure seemed to improve the OT tests by reducing the variability of the tests. The peak loads were repeatable and while the repeatbility of the numbers of cycles to failure did improve, they were still not considered reliable enough.

Based on the results from the multi-laboratory study and the marginal improvement to the repeatability of the number of cycles to failure with the modified experimental setup, it was concluded that the current failure criterion needed further investigation.

2.3 NUMBER OF CYCLES TO FAILURE AS A PERFORMANCE MEASURE

The average load-displacement curve from the monotonic OT tests described above is compared with the average load-displacement curve of the first cycle of the cyclic OT tests in Figure 2.3. A similar pattern is observed from both tests up to a displacement of 0.025 in. Both curves exhibit that the specimens were loaded into the post-failure zones. The specimens subjected to the cyclic OT had already experienced significant deformations past the peak load at the end of the first cycle.

Figure 2.4 presents the typical hysteresis loops for a Type C mix using the cyclic OT test. There is a clear distinction between the first and the subsequent cycles. The differences in the shapes of the first and the second cycles suggest that the high deformation levels applied during the first cycle has severely damaged the specimen. The hysteresis loop from the tenth cycle is

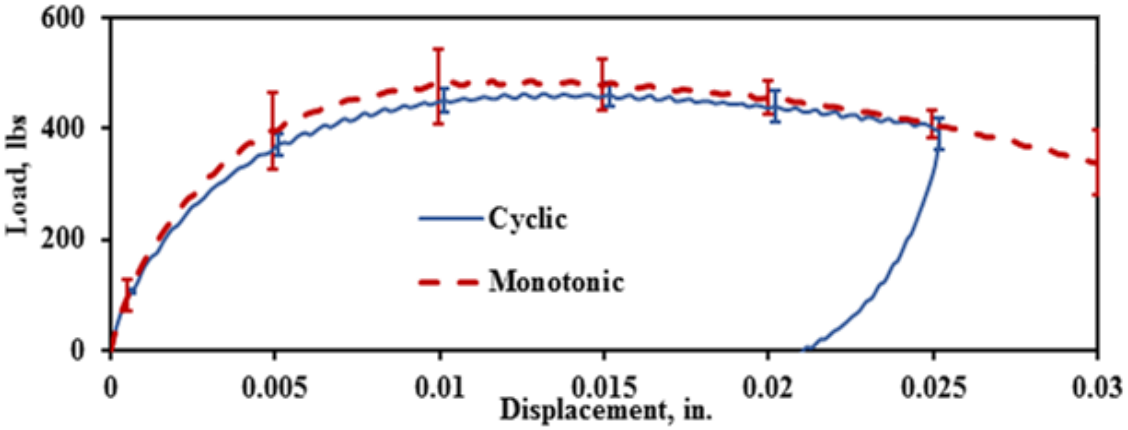

Figure 2.3: Superposition of Monotonic and Cyclic Load Displacement Curves

considered as a classical indication of a severely damaged (failed) specimen. The variability of the number of cycles to failure can be attributed to this matter amongst others. As such, the first cycle is essentially a severe crack initiation step, and the other cycles contribute to the crack propagation.

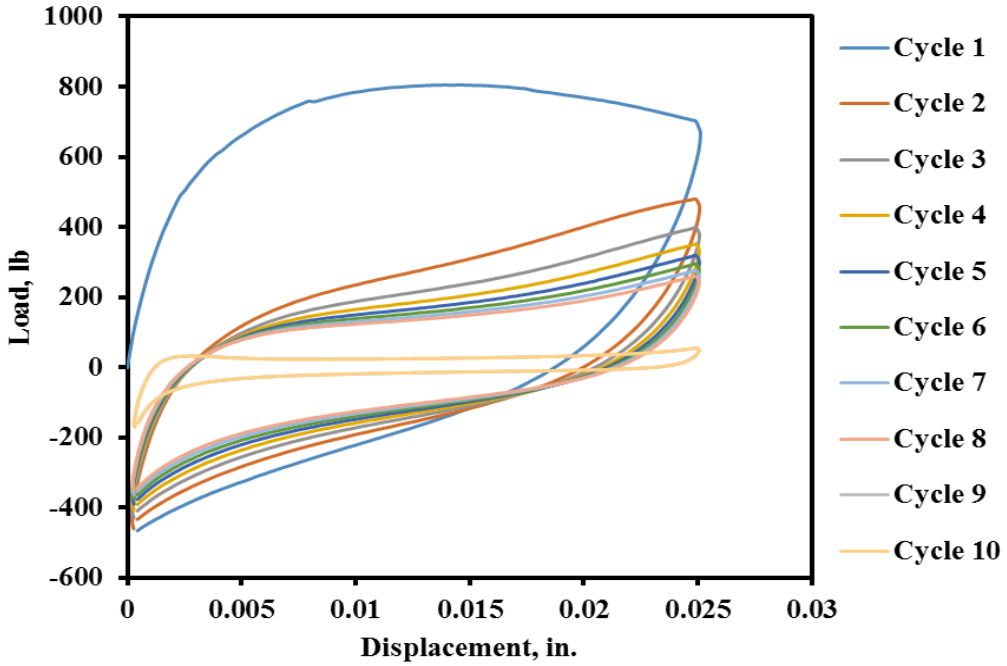

Figure 2.4: Shapes of Hysteresis Loops

Figure 2.5 presents the peak load vs. the number of cycles for the thirty two Type C specimens tested at UTEP. The data exhibit significant dispersion. Figure 2.6 shows the results from two of the specimens tested. Despite the similarity of the load versus load cycle curves, the

numbers of cycles to failure based on the 93% load reduction criterion are significantly different. This is an indication that alternative methods or parameters should be investigated as a replacement for the number of cycles to failure.

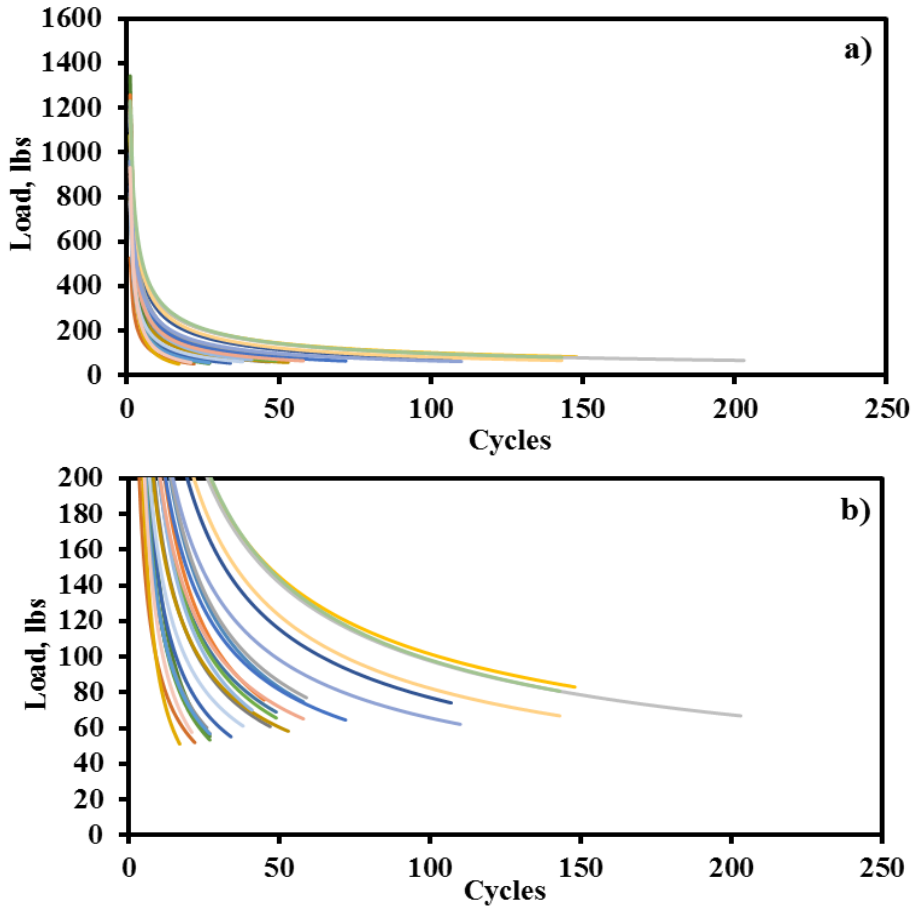

Figure 2.5: Load Reduction Curves: a) Complete and b) Zoomed Graph

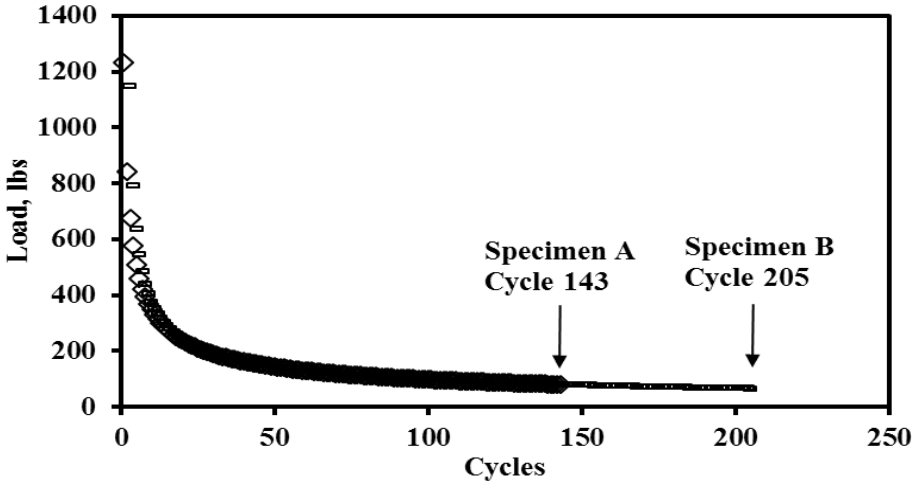

Figure 2.6: Specimens with Similar Load Reduction Curves

Chapter 3: Alternative Performance Indicators

The main purpose of this chapter was to analyze alternative cracking test methods and parameters to find a surrogate performance indicator. This chapter describes a correlation analysis performed with the indirect tensile (IDT) test and OT-Fracture. Also an evaluation on alternatives parameters obtained from the OT and an alternative analysis method.

3.1 INVESTIGATION OF ALTERNATIVE CRACKING METHODS

Walubita et al (2013) compared the OT tests with alternative crack test methods such as the traditional indirect tensile (IDT) test. They reported that the IDT parameters were repeatable with COV values shown in Table 3.1. A correlation analysis among the parameters measured with the OT, OT-Fracture and IDT tests was performed in search of an alternative parameter to screen the cracking resistance of the HMA mixes.

Table 3.1: Summary of IDT Results, Walubita et al. (2013)

Mix Type	Fracture Energy, G_f		Tensile Strength, σ_t		Strain, ε_t	FE Index
	(J/m^2)	($lb\text{-}in./in.^2$)	(psi)	(MPa)	(mm/mm)	
Type B	136 (2.3%)	0.779 (2.3%)	103 (3.8%)	0.710 (3.8%)	0.0149 (9.9%)	1.88 (11.8%)
Type D	193 (8.1%)	1.101 (8.1%)	127 (3.7%)	0.876 (3.7%)	0.0190 (19.4%)	2.76 (24.4%)
CAM	226 (5.2%)	1.290 (5.2%)	79 (2.0%)	0.547 (2.0%)	0.0340 (4.1%)	9.21 (10.0%)

*Values in parenthesis are the coefficients of variation (COV)

Research project 0-6658, sponsored by TxDOT, contains a data storage system (DSS) that at the time of this study was populated with close to 51 pavement sections (UTEP 29 – TTI 22 sections) with 11 different mix types as shown in Table 3.2. The DSS contains the most relevant parameters for fatigue cracking performance of the HMA mixes measured with the IDT, OT-Fracture and OT tests. The OT data in the DSS includes a number of parameters including the number of cycles to failure, the peak load and the last load registered. The OT-Fracture tests are

conducted up to a displacement of 0.017 in. for 100 cycles to estimate the fracture parameters. The parameters computed for the OT-Fracture tests are the peak load, the last load, the modulus of elasticity, the number of cycles (if failure is reached before 100 cycles), and the fracture parameters A and n. The information stored from the IDT tests includes the failure load, the displacement at failure, the strength and the modulus of elasticity. Apart from the parameters measured with the three proposed tests, the DSS also contains information about the source of the mixes such as the mix type, the binder performance grade, the layer type, the climatic region, and the county.

Table 3.2: Total number of Sections Used for Correlation Analysis

Mix Type	**Number of sections**
Type B	5
Type C	14
Type D	15
Type F	2
CAM	1
CMHB-F	4
PFC	1
SMA	4
SPC	1
SP-D	1
TOM	3
Total	**51**

The relationships among the OT cycles and the other parameters independent of the mix type were studied first. For example, Figure 3.1 shows the variations of the IDT strength with the OT number of cycles. In general, the number of OT cycles was not correlated to any of parameters mentioned above.

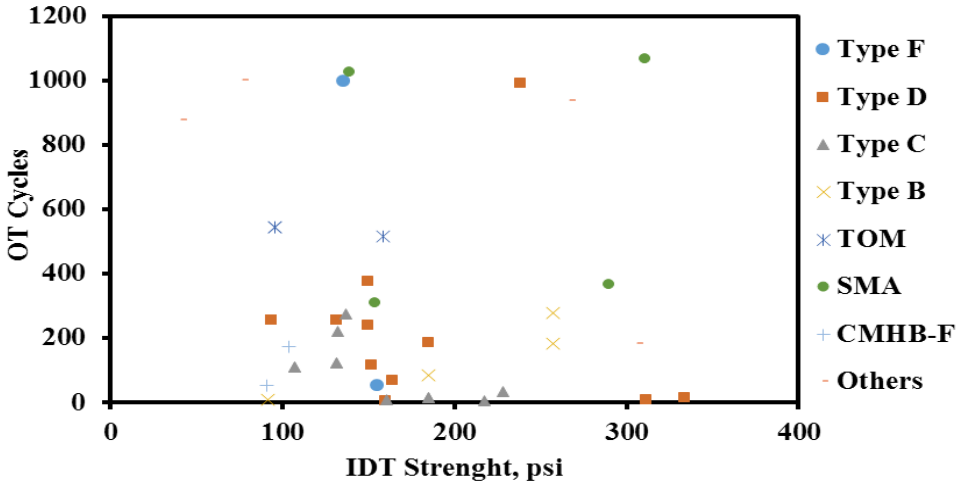

Figure 3.1: Correlation of OT Number of cycles with IDT Strength

The next step was to determine whether the OT cycles was correlated to any other parameter on the individual mix basis. The results of the correlation analyses for Type D mixes are summarized in Table 3.3 as an example, while the results from other mixes with more than three samples can be found in Appendix B. Since each test method requires different replicate tests, the average of the results for each test method was used. A good correlation, which was defined as exhibiting an absolute correlation coefficient greater than 0.60, was not observed among any of the parameters for this mix. The number of cycles did not strongly correlate with any of the available parameters.

Table 3.3: Correlation Table of Type D (15 Sections)

	Parameter	**OT**			**OT-Fracture**				
		Max. Load	No. of Cycles	Last Load	Max. Load	No. of Cycles	OT-E (Modulus)	*A*	*n*
IDT	Maximum Load	0.1	-0.1	0.1	0.1	0.7	0.1	-0.4	0.1
	Displacement at Failure	-0.1	0.0	-0.1	0.1	-0.3	0.1	-0.2	-0.1
	Strength	-0.1	0.2	0.0	-0.3	0.1	-0.3	0.3	-0.1
	Failure Strain	-0.1	0.0	-0.1	0.1	-0.3	0.1	-0.2	-0.1
	Modulus	-0.3	-0.1	-0.3	0.2	0.5	0.2	0.4	0.4
OT-Fracture	Maximum Load	0.4	-0.5	0.3					
	No. of Cycles	-0.3	0.2	-0.2					
	OT-E (Modulus)	0.4	-0.5	0.3					
	A	-0.1	-0.1	-0.1					
	n	0.8	-0.3	0.7					

The correlations between the IDT strength and the OT maximum load and OT-Fracture maximum load are depicted in Figure 3.2. The maximum loads from the two OT test methods were weakly related to the IDT strength.

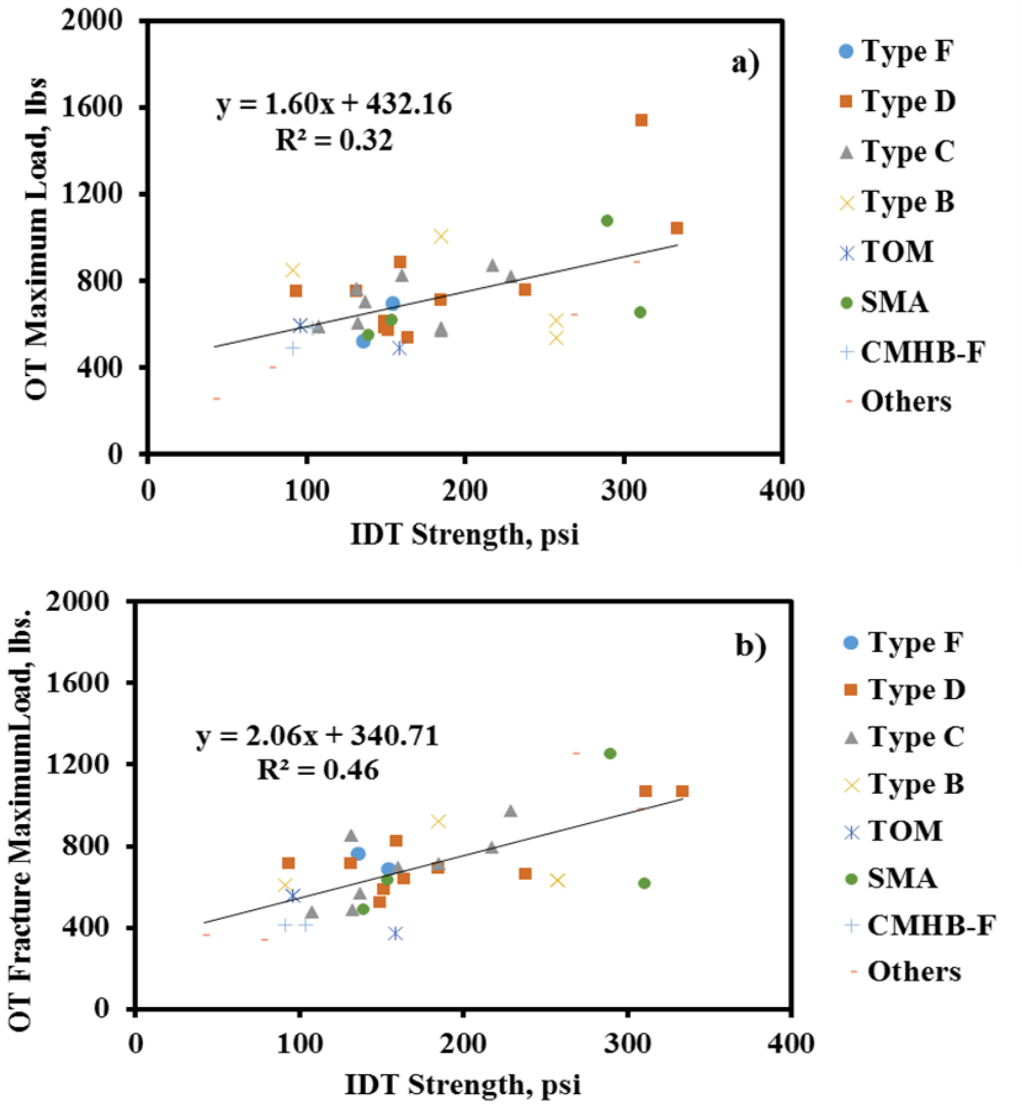

Figure 3.2: Correlation of IDT Strength to: a) OT Maximum Load and b) OT-Fracture Maximum Load

Other parameter used in the correlation analysis was the modulus of elasticity (hereafter, OT-E) obtained from the OT-Fracture and the IDT strength. The modulus of elasticity is defined as the slope of the linear portion (elastic range) of the stress-strain curve. As shown in Figure 3.3,

the two parameters follow the same trend with a moderate degree of correlation. The other correlation graphs are presented in Appendix B.

As shown in Figure 3.4, a good correlation was encountered between the OT maximum load and the IDT modulus for Type C mixes only. Such trends were not obvious for the other HMA mix types.

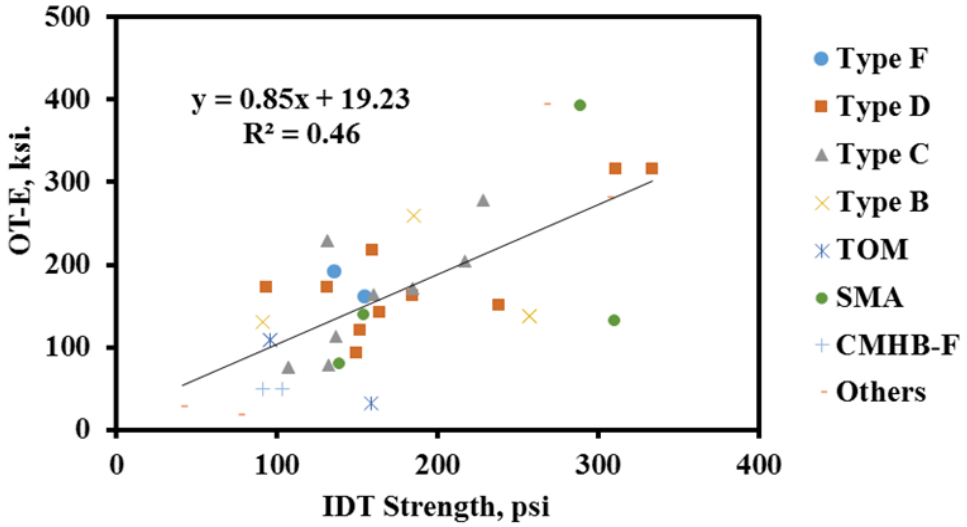

Figure 3.3: Comparison between OT-E and IDT Strength Parameters

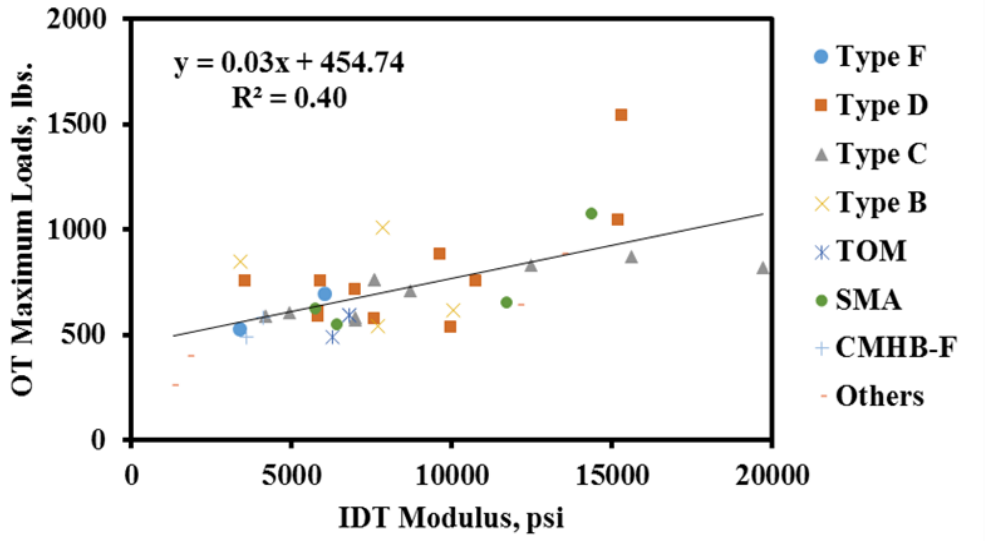

Figure 3.4: IDT Modulus Compared with OT Maximum Load

To have an overall understanding of the potential to correlate the number of OT cycles with other fatigue cracking parameters, an analysis was performed considering all mixes. Table 3.4 presents the results of the correlation analysis for all mix types. A parameter that could consistently and reliably estimate the performance of the number of OT cycles was not encountered.

Table 3.4: Correlation Table of All the Mixes (51 Sections)

	All Mixes	OT			OT-Fracture				
		Max. Load	No. of Cycles	Last Load	Max. Load	No. of Cycles	OT-E (Modulus)	*A*	*n*
IDT	Failure Load	0.4	-0.1	0.4	0.2	0.2	0.2	-0.3	0.0
	Displacement at Failure	-0.4	0.4	-0.2	-0.3	0.0	-0.3	-0.1	0.1
	Strength	0.3	0.1	0.4	0.0	0.1	0.0	0.0	0.0
	Failure Strain	-0.4	0.4	-0.2	-0.3	0.0	-0.3	-0.1	0.1
	Modulus	0.2	-0.3	0.0	0.3	0.1	0.3	0.1	-0.2
OT-Fracture	Maximum Load	0.4	-0.4	0.2					
	No. of cycles	-0.3	0.3	-0.1					
	OT-E (Modulus)	0.4	-0.4	0.2					
	A	0.0	-0.1	0.0					
	n	0.4	-0.1	0.4					

3.2 INVESTIGATION OF ALTERNATIVE PARAMETERS MEASURED WITH OT TEST

Since a promising correlation among the cracking parameters of other tests could not be found, it was decided to investigate alternative parameters from the OT test. The results from the multi-laboratory study provided a vast source of data that were analyzed for identifying a potentially reliable surrogate parameter.

The first focus was on the information from the first cycle hysteresis loop. Figure 3.5 illustrates the alternative parameters considered. These parameters can be described as:

1) **Maximum load** - the highest load obtained from the first cycle. This load resulted in the initial cracking of the OT specimen.
2) **Load at maximum displacement** - the load registered at the maximum displacement (0.025 in.) of the first cycle.

3) **Displacement at maximum load** - the displacement at which the maximum load is reached during the first cycle.

4) **Initial slope** - obtained from the linear portion of the hysteresis loop of the first cycle.

5) **Displacement at zero load -** the displacement when the load is zero during the unloading time.

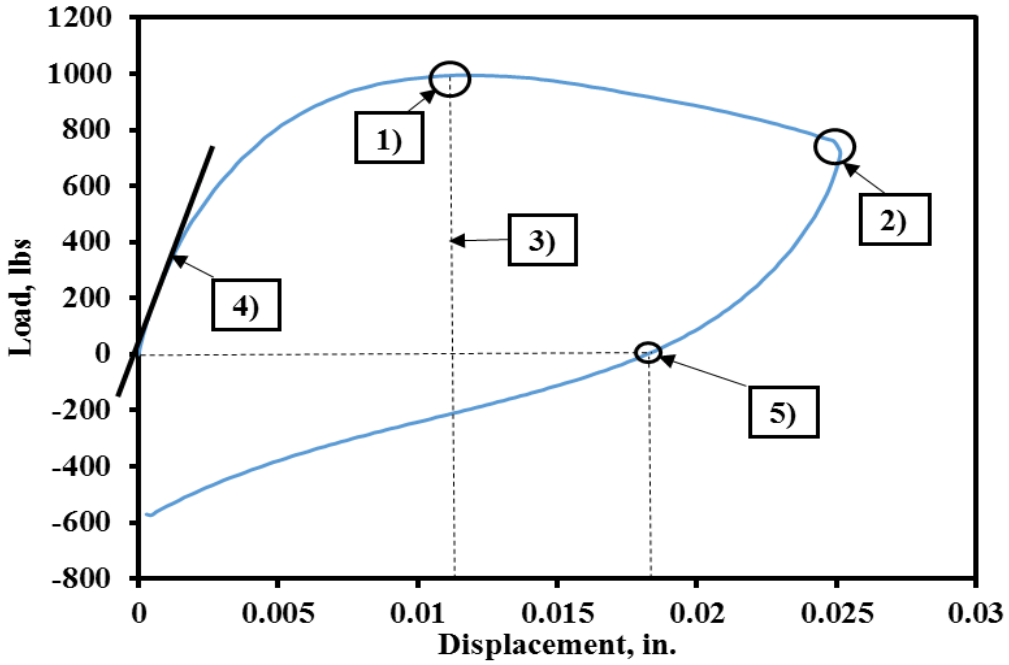

Figure 3.5: Graphical Representation of Alternative Parameters (Load and Displacement)

The area inside the hysteresis loop was also analyzed in four parts. In Figure 3.6, the three parts of the hysteresis loop area are identified with the fourth being the total area. The parameters involving the area of the hysteresis loop are desribed as follows:

1) **Loading area** – the area below the loading curve of the hysteresis loop up to the maximum displacement (0.025 in.)

2) **Unloading area –** the area below the unloading curve of the hysteresis loop from the maximum displacement to the displacement at zero load.

3) **Compressive area –** the area of the unloading curve of the hysteresis loop from the displacement at zero load to the zero displacement.

4) **Total curve area –** the sum of the areas at each stage of the hysteresis loop. The sum of the three mentioned areas. The compressive area is added to the difference between the loading and unloading area.

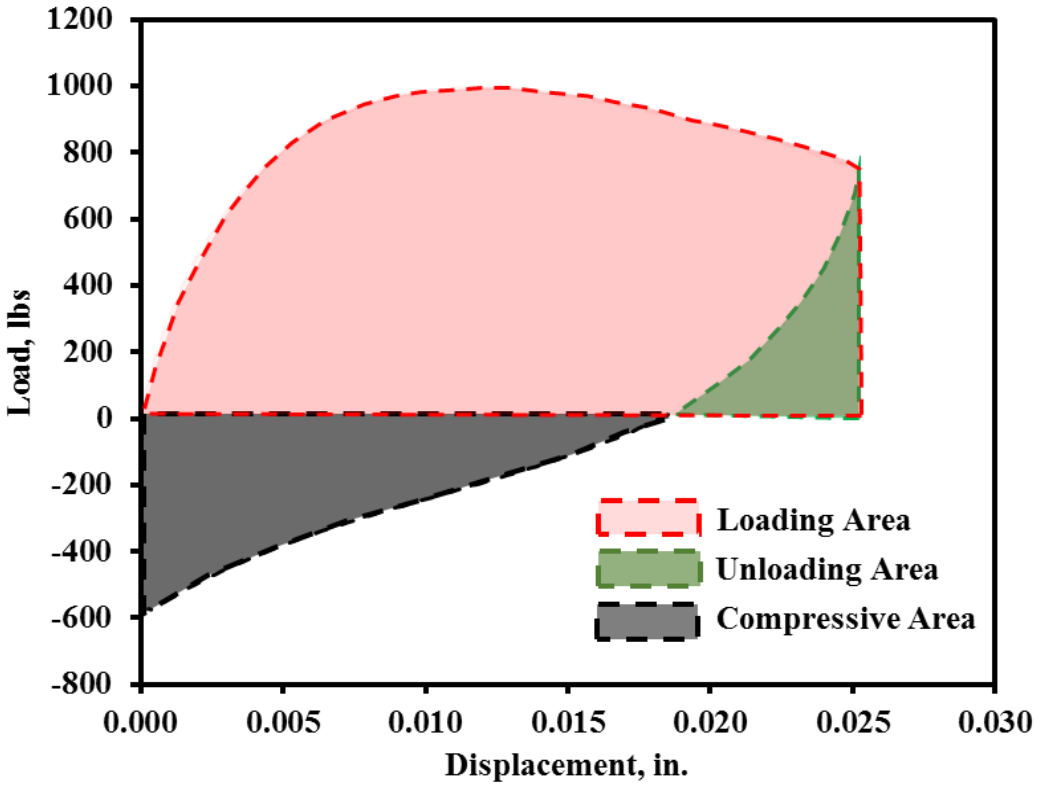

Figure 3.6: Graphical Representation of Alternative Parameters (Areas)

The measured OT parameters from the specimens tested in the multi-laboratory study were analyzed first. Since the results from the UTEP and TxDOT laboratories were similar, only the results from the thirty two specimens tested at UTEP were considered. Table 3.5 shows the results from the twenty six of the thirty two Type C specimens tested at UTEP. Six specimens were discarded from the mix since the raw data were noisy. The numbers of OT cycles to failure were also added to the analysis for comparison purposes.

Table 3.5: Summary of Results of the Alternative Parameters (26 Type C Mix Specimens)

Parameters	Average	Median	Standard Deviation	COV
Maximum Load, lbs	849	854	53	6%
Displacement at Max. Load, in.	0.013	0.013	0.002	12%
Load at Max. Displacement, lbs	683	703	62	9%
Initial Slope, lbs/in.	192339	174739	56628	29%
Displacement at Zero Load, in.	0.019	0.019	0.000	2%
Loading Area, lbs-in.	18.0	17.9	1.1	6%
Unloading Area, lbs-in.	-1.2	-1.3	0.2	17%
Compressive Area, lbs-in.	4.2	4.2	0.2	5%
Total Area, lbs-in.	21.0	21.0	1.1	5%
Number of Cycles	57	43	47	82%

In consultation with TxDOT, a COV equal or less than 20% was considered to correspond to an acceptable repeatability. As reflected in Table 3.5, all parameters, except the initial slope and the number of cycles at failure, yielded COVs that were less than 20%. The total area, which is usually referred to as the dissipated energy, was identified as a promising parameter with consistent results and low COV. Similarly, the loading area, which represents the energy required for fracturing the specimen, showed low COV value.

3.3 ALTERNATIVE ANALYSIS METHOD

A crack resistance mix should ideally exhibit the following two characteristics:

1. The mix should be tough enough so that it would not permit easily the initiation of a crack. This means that during the first cycle of OT test, the peak load should be as high as possible, and the displacement at peak should be as large as possible, and
2. The mix should be flexible enough so that it would attenuate the rate of the propagation of the crack after it is initiated. This means that from the second cycle on, the rate of loss of load should be rather gradual.

Figure 2.4 clearly supports the distinct differences between the first and subsequent cycles. An approach that considers the two stages of the OT tests (i.e., the crack initiation during the first cycle and the crack propagation during the subsequent cycles) was considered.

3.3.1 Crack Initiation

Walubita et al. (2013) introduced different fracture parameters to characterize the cracking resistance of different mixes using the OT in the monotonic loading mode. In general, the area under the hysteresis loop was considered as crucial to compute the fracture parameters that characterize the crack initiation stage. The fracture energy represents the energy required to fracture a specimen. The dissipated energy is considered as the energy released during the loading and unloading stages of each cycle (in this case the first cycle). The difference between the two fracture parameters is the portion of the area required from the hysteresis loop.

The area within the hysteresis loop is considered for estimating the dissipated energy (see Figure 3.7). Equation 1 can be used to calculate the dissipated energy.

$$G_d = \frac{Wd}{A} \quad (1)$$

where G_d = Dissipated Energy (lbs-in/in^2), W_d = area within the hysteresis loop, A = area of the cracked section which is considered as the specimen thickness multiplied by the width of the specimen (1.5 in. x 3.0 in.)

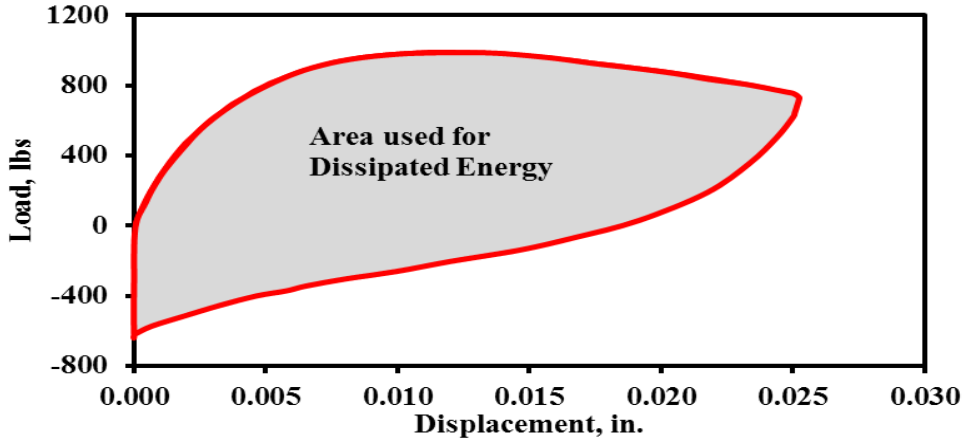

Figure 3.7: Area Used for the Calculation of Dissipated Energy

The COV of the dissipated energy for the twenty six Type C specimens was about 5%. One concern with the dissipated energy in the context of the OT is that it also involves the compressive area, which does not seem to be related to or explainable with the fracture mechanic principles. Since both the cyclic and monotonic OT tests apply deformations past the peak strength, it can be assumed that the fracture energy, G_f, can be reliably calculated from the cyclic OT test using:

$$G_f = \frac{Wf}{A} \tag{2}$$

where W_f = the area considered for the calculation of the fracture energy is shown in Figure 3.7. The COV of the fracture energy calculated for the twenty six Type C specimens was 12%.

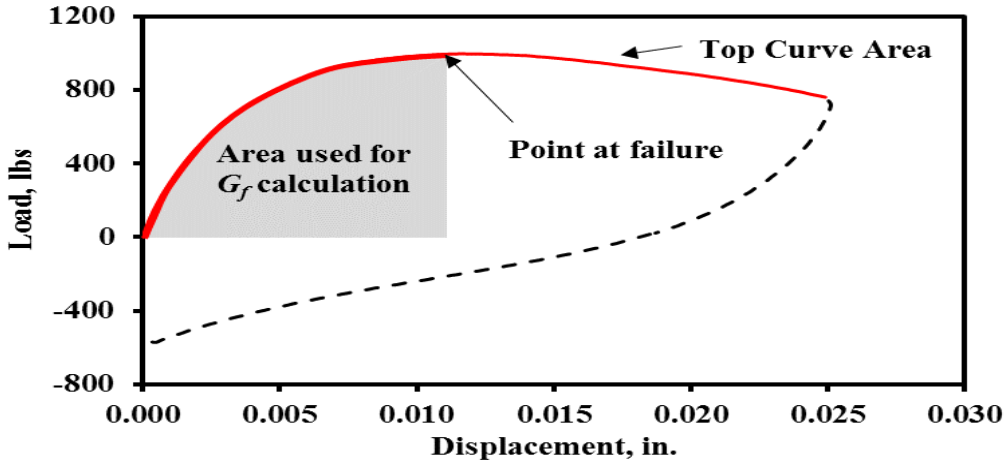

Figure 3.8 Area Used for Calculation of fracture Energy

3.3.2 Crack Propagation

For the crack propagation stage of the OT test, the loading cycles two and up were considered. Figure 3.9 presents the variation of the maximum peak load against the number of OT cycles. The specimen reached the 93% load reduction criterion relative to the first cycle peak load after 30 cycles. About 50% of the load reduction occurred between the first and second cycle.

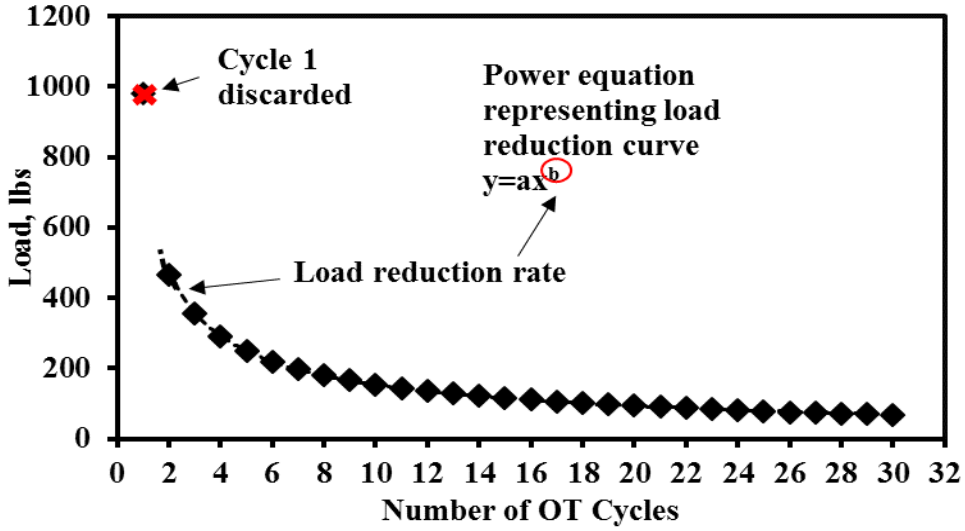

Figure 3.9: Load Reduction Rate Graphical Representation

The crack propagation was quantified by first fitting a power equation to the second and subsequent data points. The reason for the curve fitting was to minimize the experimental uncertainties related to the load cell. A load cell with a capacity of either 5000 or 2000 lbs is often installed in the OT device. Considering an optimistic precision of 0.1% for the load cell, the reported loads are within 2 to 5 lbs of the actual values. Considering that the test has to be continued until the load decreases by 93%, the level of uncertainty in the measured loads is up to 10% of the actual value. The curve fitting, which normally yields R^2 values close to 1, is meant to smooth the uncertainties in the load measurements. Instead of the 93% of the maximum load from the first cycle, the power coefficient of the power equation is interpreted as the load reduction rate. This is identified as the b-coefficient of the power curve presented in Figure 3.9.

To compare the results of the load reduction curves more consistently, the loads were normalized by the maximum load of the second cycle (instead of the first cycle). Figure 3.10 shows the normalized load reduction curves obtained from the twenty six specimens. The curves diverge significantly for normalized loads of less than 25%; hence significant dispersion in the number of cycles to failure.

Figure 3.11 shows the average and median trends of the twenty six specimens tested. The abscissas of the graphs are changed to logarithmic scale to provide a better visualization of the normalized load reduction curves. The error bars, which correspond to ± one standard deviation, are added to show the deviations of the data from the average and median. In these figure, cycle 1 corresponds to the second OT cycle since the first cycle was associated with the initiation of the crack (not the propagation of the crack). Also under the curve-fitting scheme the constant associated with the power curve is also equal to unity (100%), while the power term is always negative.

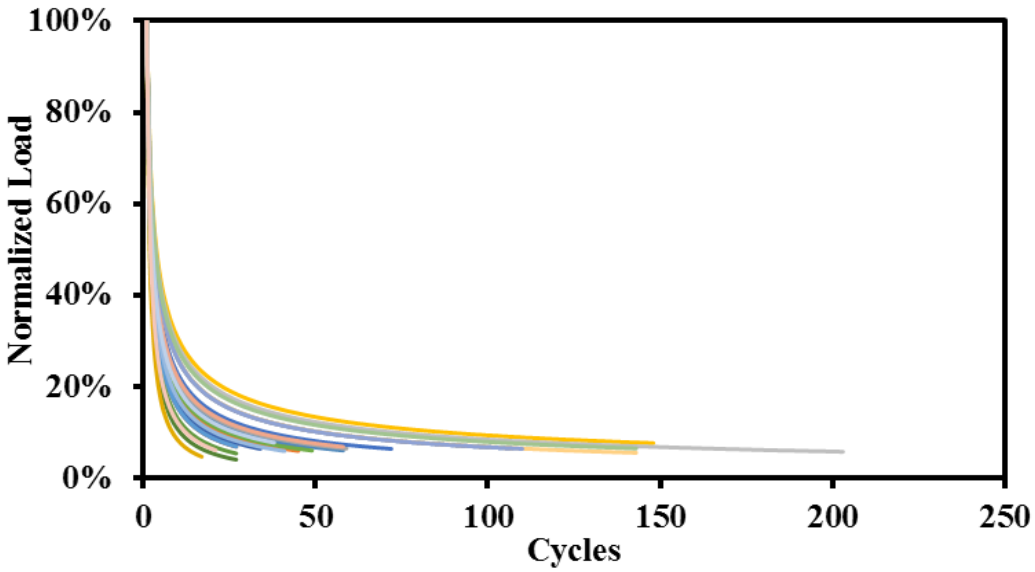

Figure 3.10: Normalized Load versus Cycles

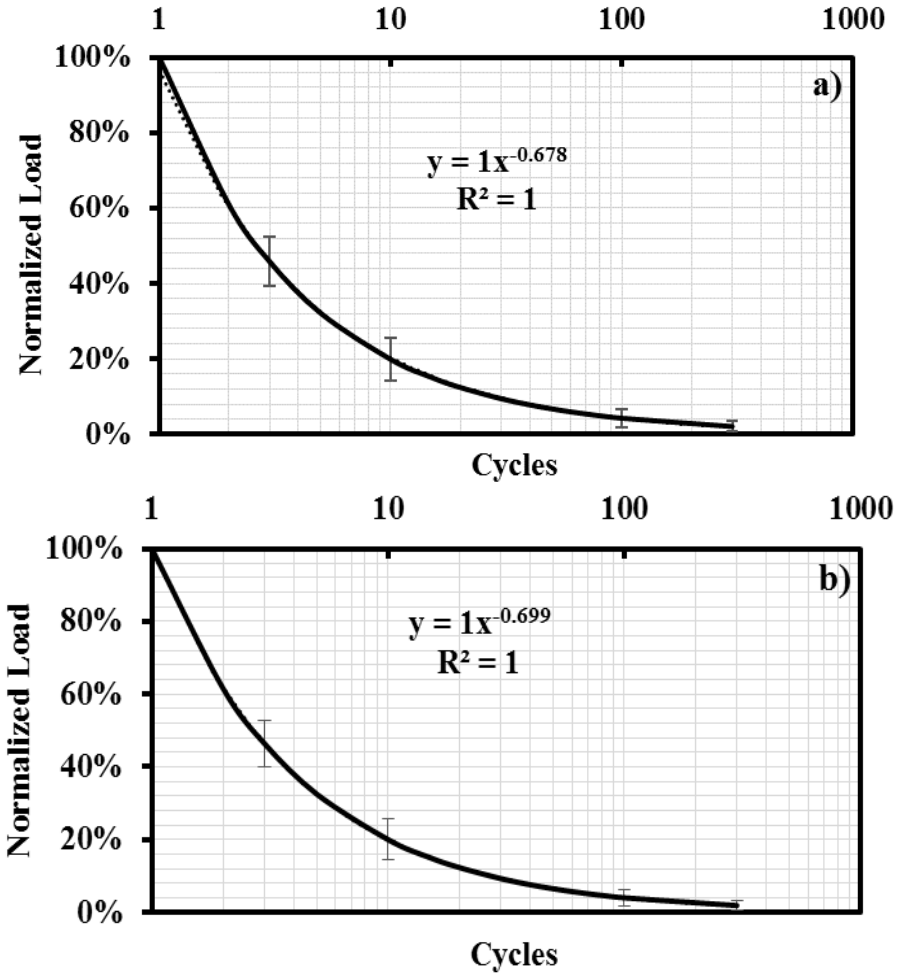

Figure 3.11: Normalized Load Reduction Curves for a Type C Mix: a) Average and b) Median

Using the fit parameters of the normalized load reduction curves, instead of the number of cycles to failure seemed promising as an alternative approach for estimating the resistance of the HMA specimens to cracking. The preliminary conclusions drawn from this activity were:

- the maximum load, displacement at the maximum load, and the area under the hysteresis loop from the first cycle may explain the crack initiation, and
- the fit parameter from the normalized load reduction curve may be a candidate for assessing the crack propagation resistance of the HMA specimens in a more consistent manner.

Chapter 4: Assessment of Alternative Analysis Method

This chapter shows the assessment of the alternative analysis method, implementing data of different HMA mixes provided by TxDOT. The properties of the HMA mixes are presented on this chapter. Finally, the results obtained using the different HMA mixes are shown and discussed.

4.1 CHARACTERISTICS OF HMA MIXES

To evaluate the potential of the approach above, the data from over 212 OT tests performed by TxDOT in the previous several years were obtained. Table 4.1 provides the numbers of test results that were available by the mix type. A database that contained the relevant information about the OT specimens such as the date tested, performance grade (PG) of the binder, asphalt content (AC), anti-stripping content and asphalt source was also available. Only the data from 2012 through 2015 that corresponded to the latest Tex 248-F test procedure were used.

Table 4.1: Mixes Used for the Alternative Approach

Mix Type	Sample Size
Type C (Coarse Surface)	30
Crack Attenuating Mix (CAM)	35
Type D (Fine Surface)	26
Thin Overlay Mix (TOM)	20
Superpave-C (SP-C)	33
Stone Matrix Asphalt (SMA-D)	20
Stone Matrix Asphalt (SMA-F)	12
Permeable Friction Course (PFC-F)	12
Superpave-D (SP-D)	24
Total	**212**

The properties of the mixes are shown in Tables 4.2 and 4.3. The CAM mixes contained asphalt content between 7.0% and 7.9%, implying a more elastic mix. Type C, Type D and SP-C

Table 4.2: Mix Characteristics of the Data Provided by TxDOT

Mix Type	Asphalt Content (%)					Performance Grade				Anti-Strip Usage					
										Lime	Liquid				
	4.0-4.9	5.0-5.9	6.0-6.9	7.0-7.9	Not Specified	PG 64-22	PG 70-22	PG 76-22	Not Specified	1%	0.3%	0.5%	0.75%	1%	None Used
Type C (Coarse Surface)	15	6			9	9	12	6	3	9				3	18
Crack Attenuating Mix (CAM)				18	17			15	20	12		3			20
Type D (Fine Surface)	6	18			2		15	8	3	12					14
Thin Overlay Mix (TOM)			15	3	2		5	9	6	9	6				5
Superpave-C (SP-C)	3	24	3		3	3	21	6	3						33
Stone Matrix Asphalt (SMA-D)			15		5			17	3	3			6		11
Stone Matrix Asphalt (SMA-F)			12					6	6	12					
Permeable Friction Course (PFC-F)		3	3		6			12		6			3		3
Superpave-D (SP-D)		12	3		9	6	12	6		6			3	3	10

Table 4.3: Mixes Providers and Year of Test

Mix Type	Asphalt Source										Year Tested			
	Alon	**Century Asphalt**	**Gary-Williams**	**Heartland**	**Jebro**	**Lion**	**Martin Asphalt**	**Wright**	**Nustar**	**Valero**	**Not Specified**	**2012**	**2013**	**2014**	**2015**
Type C (Coarse Surface)		3	3		3	3				6	12	9	15	6	
Crack Attenuating Mix (CAM)				3			6	9	3	3	11	35			
Type D (Fine Surface)						3	3			15	5	8	18		
Thin Overlay Mix (TOM)					6	3				9	2	12		8	
Superpave-C (SP-C)	12					6				3	12	15		9	9
Stone Matrix Asphalt (SMA-D)				3	3	6	3				5			12	8
Stone Matrix Asphalt (SMA-F)					12									12	
Permeable Friction Course (PFC-F)										3	9				12
Superpave-D (SP-D)	12			3						6	3			21	3

used asphalt contents ranging from 4.0% to 5.9%. The most common binder was PG 76-22. About half of the specimens did not use anti-stripping agents, while around one fourth used 1% lime.

4.2 HMA MIXES EVALUATION

The normalized load reduction curves were generated for all available specimens. As an example, the results from the CAM mixes are shown in Figure 4.1a. The curves that represented the average and median of the normalized load reduction curves are also presented in the figure. The curve associated with a 93% load reduction that will follow the power equation is also shown. For this mix type, most curves associated with individual mixes lie above the curve corresponding to the 93% failure criterion. Figure 4.1b shows the average trend for all the CAM mixes with error bars representing ±1 standard deviations for several different cycles. The abscissa of that figure is converted to logarithmic scale. Three trend lines associated with 100, 300 and 1000 cycles to reach a load reduction of 93% are also shown. Since the average curve is above all the three failure criteria, the CAM specimens tested seem crack resistant.

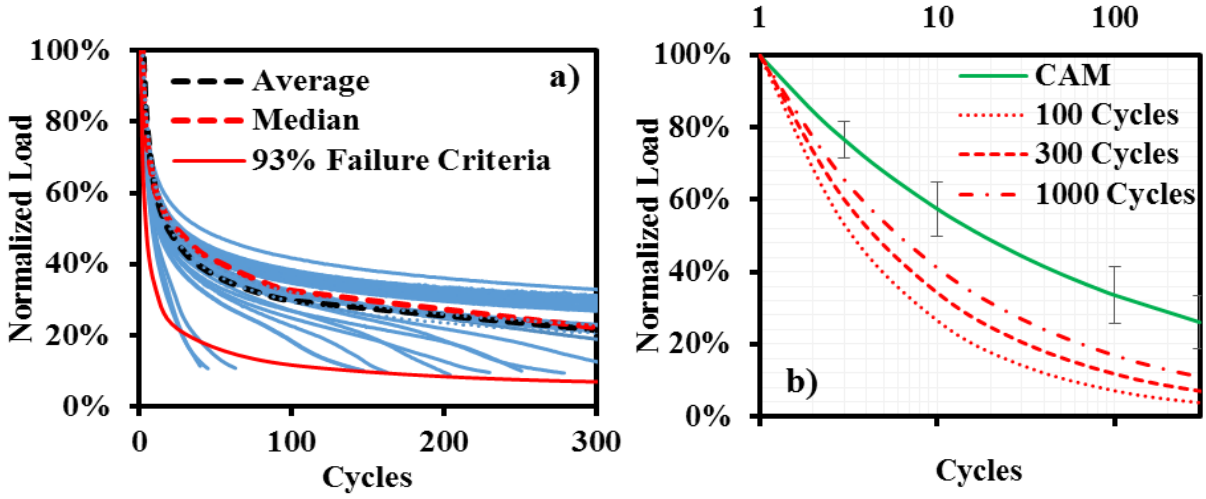

Figure 4.1: a) Normalized Load Reduction curves of CAM Mix and b) CAM Average

Figure 4.2 presents the average normalized load reduction curves for all mix type superimposed on to the current OT failure criterion of 300 cycles as well as criteria based on 100

and 1000 cycles. Error bars are added to the average curves to demonstrate the uncertainties associated with different mixes. Appendix C contains the same procedure but showing the median line of each mix type. To comparatively evaluate the performance of the different HMA mixes, the average trends for all mix types are superimposed on the three failure criteria in Figure 4.3. The average curves for the CAM, TOM and PFC mixes always lie above the failure criterion curve of 300 cycles. Almost all Type D mixes performed poorly as per current criterion. The other mixes sometimes passed and sometimes failed the current criterion.

Based on this study, a data interpretation method that involves the two phases of the OT test, crack initiation, and crack propagation, was proposed. The surrogate parameter for quantifying the crack initiation is the fracture energy. The higher that value is, the more energy it will take to initiate the crack.

The load reduction rate, the power parameter obtained from fitting a power curve to the normalized load vs. number of cycles, was used as a surrogate for characterizing the resistance to cracking during the crack propagation. The greater the absolute value of that power is, the faster the crack propagation through the specimen will be. The power corresponding to the current criterion of 300 cycles for a 93% load reduction corresponds to -0.465 (rounded to -0.5).

As an example, the fracture energy and the load reduction rate of each CAM mix is plotted in Figure 4.4. The label for each data point is its peak load during the first cycle. Lines corresponding to the median and average load reduction rates are also added to the plot. Also shown in the figure is the line corresponding to a 93% load reduction (current failure criterion).

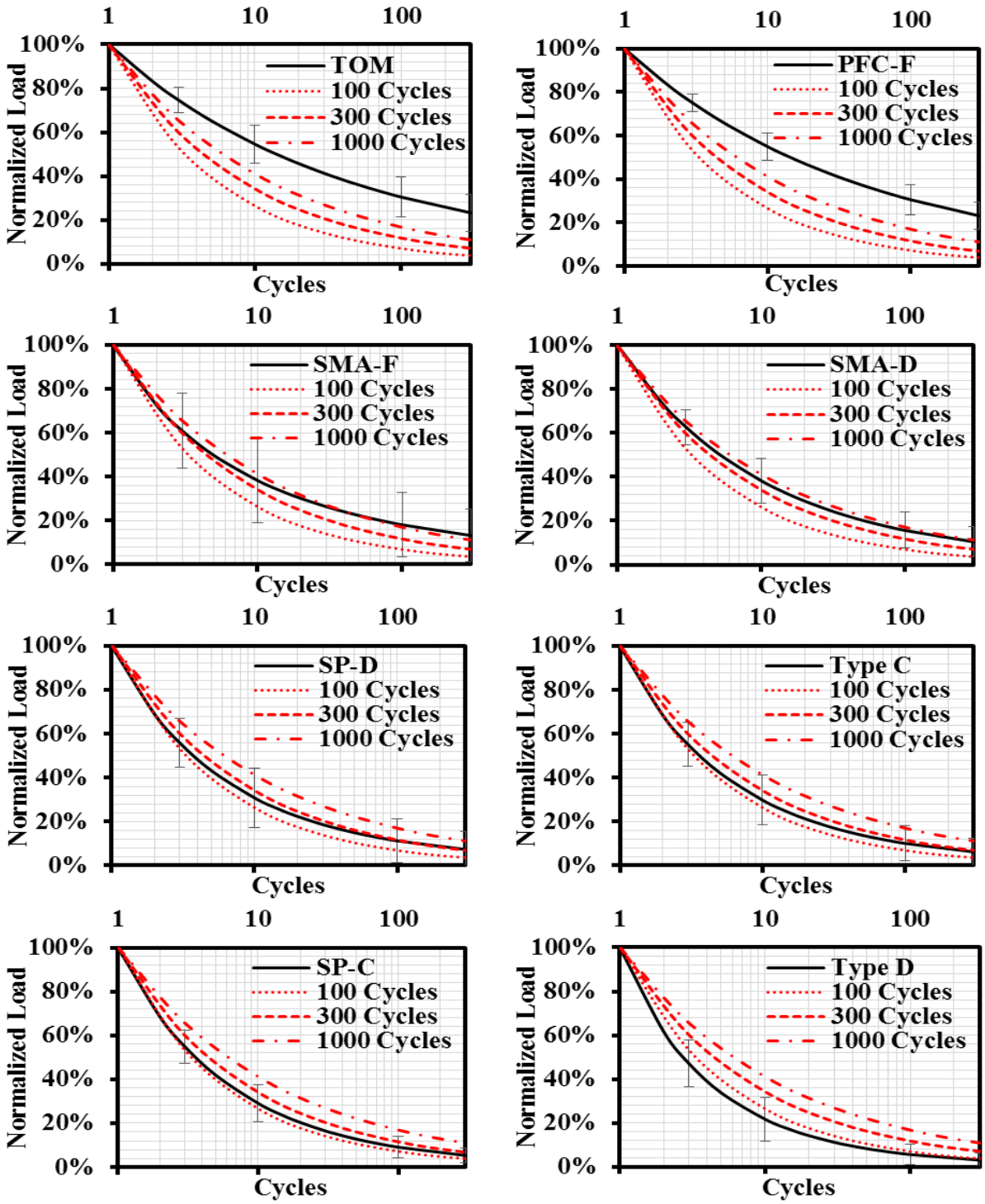

Figure 4.2: Average Lines of the Different HMA Mixes

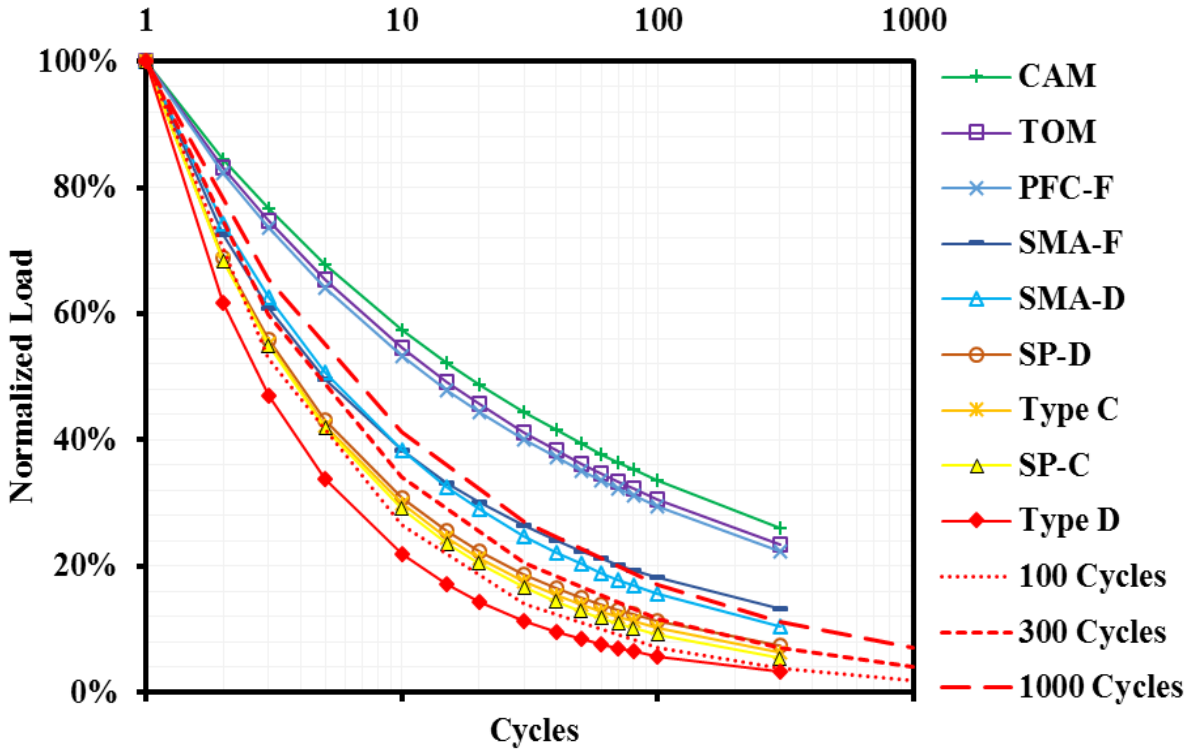

Figure 4.3: Average Curves for All HMA Mixes

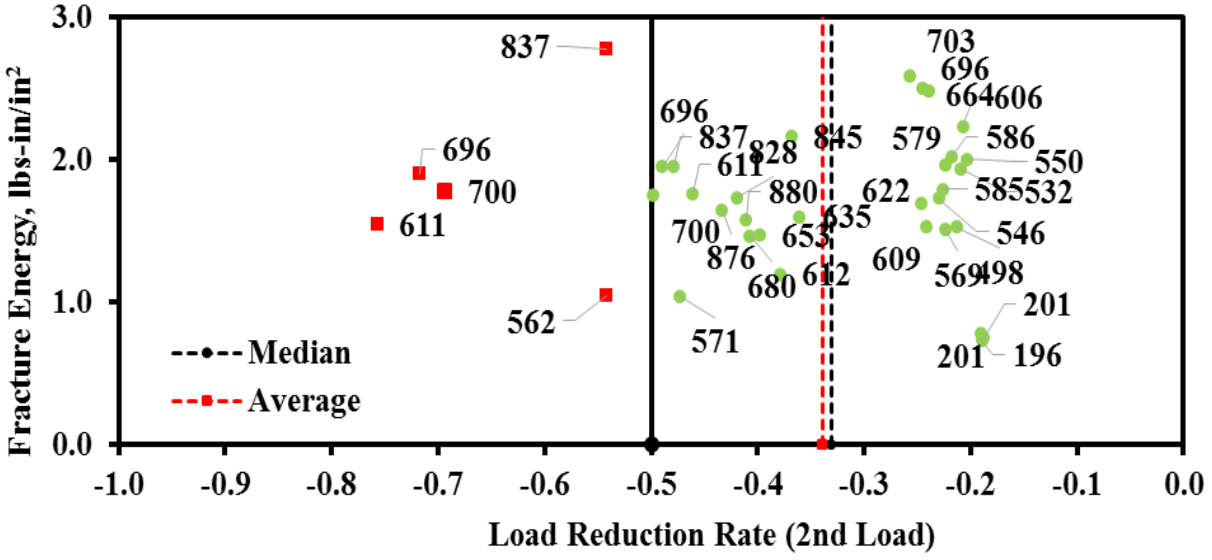

Figure 4.4: Cross Plot of Load Reduction Rate and Fracture Energy of CAM Mix

Based on the load reduction rate, two zones were identified: good crack retardants (green points) and poor crack retardants (red points).

The ordinance, the fracture energy, can also be used to judge the crack initiation potentials of the mixes. For two mixes that are good crack attenuators (say with the load reduction rate close to -0.2 in Figure 4.4), the mix with the higher fracture energy will resist the initiation (not the propagation) of the crack better than a mix with the lower fracture energy. The results for all mixes are shown in Appendix D and discussed below.

4.3 RESULTS

The interpretation of the results following the proposed process was carried out, and reported in Appendix D for each mix type. Figure 4.5 shows the box plot of the distributions of the load reduction rates and fracture energies for each mix type. According to this methodology, the best mix type is the TOM since it required more energy to initiate a crack (high fracture energy) and it was very flexible (lowest load reduction rate) after the crack was initiated. The CAM mixes are ranked as the second best because of a high average fracture energy and low reduction rate. The

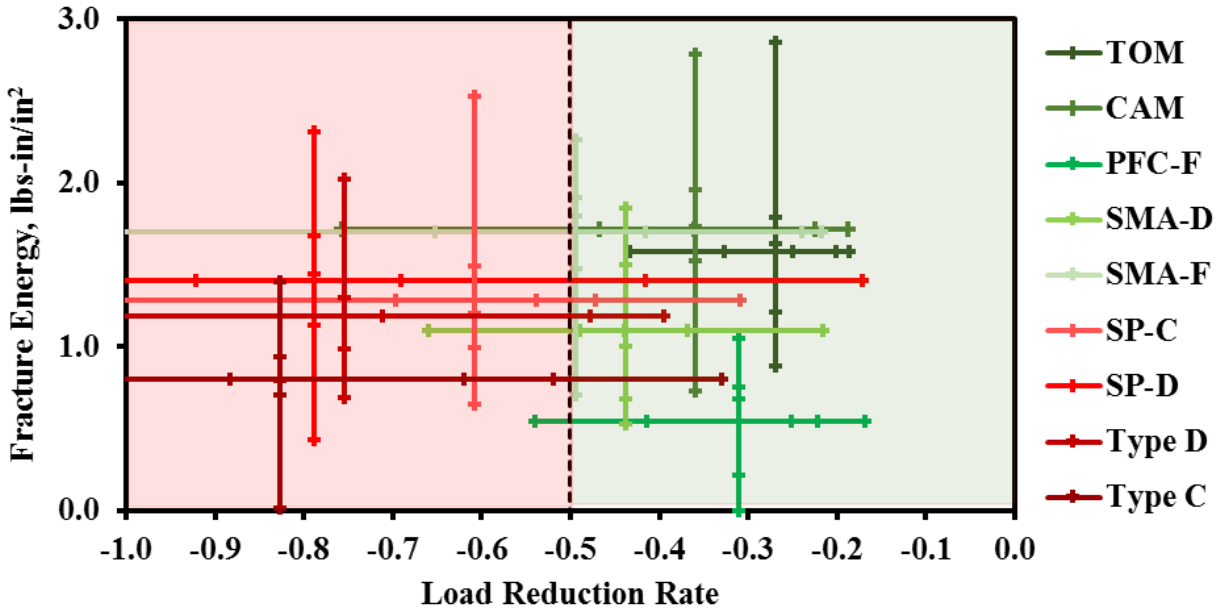

Figure 4.5: Load Reduction Rate versus Fracture Energy with All Mix Types

PFC-F mixes presented high flexibility after crack initiation, but the energy required to initiate a crack was low. On average, the Type C, Type D and SP-D mixes are ranked the worst because of the low fracture energy and high load reduction rate. However, it seems that the Type C mixes are on average more prone to initiate and propagate the cracks than any other mix.

One of the main objectives of this study was to improve the repeatability of the parameters used to characterize the cracking resistance of HMA specimens from the OT test. Each HMA mixture contained a number of sets of triplicate specimens. The average and COV of the implemented parameters and the number of cycles to failure were calculated for each set of specimens. The medians of the averages and COVs of all sets of specimens for a mix type are shown in Table 4.4. The detailed results for each mix are shown in Appendix E. The COVs of some mixes such as TOM and PFC-F that tend to last more than 1000 cycles before reaching the 93% reduction in load are not reported due to the 1000 cycle setup limit of the OT machine. As an example, the 9% COV value for the number of cycles for CAM mixes is also biased because the majority of specimens lasted at least 1000 cycles. The COVs of the fracture energies is typically less than 20% except for the PFC-F. To check this inconsistency, the hysteresis loops of PFC-F were investigated and plotted as shown in Figure 4.6. It was clear from the figure that some of the loops were atypical (see set 2 as an example). Typically, this data will be discarded. However, since only a small sample size was provide to begin with, the data were included. Further investigation on a larger sample size of PFC-F would be desirable.

Another observation on the mixes investigated was that except one case (SMA-F with COV of 23%), the COVs of the load reduction rate is 20% or less. In contract, the COVs of the number of cycles to failure for mixes that were not close to the 1000 cycles are greater than 30%.

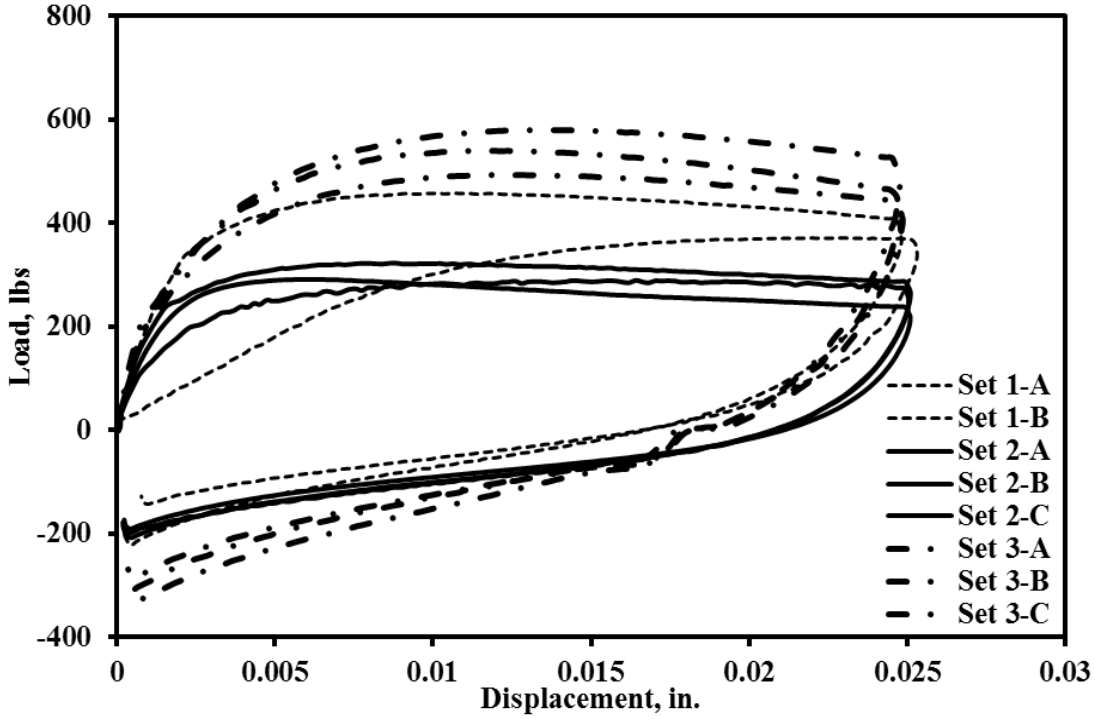

Figure 4.6: Hysteresis Loops of PFC-F Sets of Specimens

Table 4.4 Median Repeatability of Results of HMA Mixes

Mix Type	Fracture Energy, lbs-in./in.^{2}		Load Reduction Rate		Number of Cycles to Failure	
	Median	COV	Median	COV	Median	COV
TOM	1.7	14%	-0.24	12%	1000	N/A
CAM	1.8	7%	-0.32	5%	823	9%
PFC-F	0.8	35%	-0.30	18%	1000	N/A
SMA-D	0.9	10%	-0.42	19%	426	81%
SMA-F	1.6	13%	-0.42	23%	590	57%
SP-C	1.1	17%	-0.49	10%	88	38%
SP-D	1.4	11%	-0.61	20%	134	37%
Type D	1.2	9%	-0.61	11%	22	40%
Type C	0.8	16%	-0.53	11%	34	31%

Chapter 5: Summary and Conclusion

The high variability of results using the current performance indicator of the OT has been a concern for several years. The necessity to implement a surrogate parameter(s) as a performance index is very important. The objective of this thesis was to evaluate the current OT performance indicator and develop an alternate methodology to estimate the fatigue cracking performance of HMA mixes, reliable enough to be implemented as a new failure criteria for OT.

This thesis presented the current OT device used to estimate the fatigue cracking performance as well as the current performance indicator which is the number of cycles to failure. The methodology followed on this thesis was first to investigate alternative fatigue cracking methods in order to find a good correlation between parameters to implement a surrogate. The correlation analysis performed did not provide a parameter that could consistently and reliably estimate the performance of the number of cycles to failure.

Then, an investigation on alternative parameters measured with the OT was followed using a set of Type-C specimens. Promising parameters were found from this analysis showing COV values under 20%. Finally, an alternative analysis method to estimate the fatigue cracking performance was proposed, implementing the crack initiation and propagation stages of the OT test.

The alternative analysis method was evaluated by assessing nine different HMA mixes in order to delineate each of the mixes. According to the new failure criteria the TOM and CAM mixes demonstrated to have the best cracking performance by being difficult to initiate a crack as well as good crack retardants. Type C, SP-D and Type D showed to be the worst mixes by being the most prone to crack and having a fast crack propagation.

The following conclusion can be drawn from this study so far:

1. The load-displacement curves from the cyclic and monotonic OT tests illustrated that the specimens are strained past their peak loads. Conducting a cyclic test based on the current specification to estimate the cracking performance on a specimen in post-failure condition may not reliably capture the cracking properties of the HMA specimens.
2. The OT test was divided into two phases: crack initiation phase and crack propagation phase.
    - The first cycle of the cyclic OT method contributes to the initiation of the crack. The fracture energy, which corresponds to the area below the load-displacement curve up to peak load,, was selected to assess the initial cracking resistance of HMA specimens (crack initiation phase). The higher the fracture energy is, the greater the energy required to initiate the crack will be.
    - The normalized load reduction curve computed from the second and subsequent cycles was considered for discriminating the cracking resistance of mixes. This curve was normalized by the maximum load of the second cycle and fitted with a power equation to quantify the resistance of the HMA specimen to attenuate the propagation of the crack after it is initiated.
3. The repeatability of the implemented parameters used in this methodology were compared with the number of cycles to failure. The fracture energy and the load reduction rate seemed to be more repeatable than the number of cycles to failure.

The proposed methodology demonstrated to effectively distinguish between the nine mixes used in this analysis. The parameters used to describe the two stages of the OT test showed high consistency, making this new methodology a promising fatigue cracking performance indicator.

References

1. Garcia, V. and Miramontes, A. (2015) "Understanding Sources of Variability of Overlay Test Procedure". No. 16-2317, Journal of the Transportation Research Board, No. 2507, 10-18, Transportation Research Board of the National Academies, Washington D.C.

2. Germann, F. P., and Lytton, R. L. (1979). "Methodology for Predicting the Reflection Cracking Life of Asphalt Concrete Overlays." Report No. FHWA/TX-79/09+207-5, Texas Transportation Institute, College Station, Texas.

3. Ghuzlan, K. A., and Carpenter, S. H. (2003). "Traditional fatigue analysis of asphalt concrete mixtures." 82nd Annual Meeting of Transportation Research Board, CD-ROM, Washington D.C.

4. Hajj, E., Sebaaly, P., and Loria L. (2008) "Reflective cracking of flexible pavements phase II: review of analysis models and evaluation tests." Research report No. 13JF-1, Nevada Department of Transportation.

5. Hu S., Zhou, F., Scullion, T., and Leidy, J. (2012). "Calibrating and Validating Overlay Tester–Based Fatigue Cracking Model with Data from National Center for Asphalt Technology." Transportation Research Record, Journal of the Transportation Research Board, No. 2296, 57–68, Transportation Research Board of the National Academies, Washington, D.C.

6. Jacobs, M. M. J., Hopman, P. C., and Molenaar, A. A. A. (1995). "The crack growth mechanism in asphaltic mixes." HERON, 40, (3), ISSN 0046-7316.

7. Jacobs, M. M. J., Hopman, P.C., and Molenaar, A. A. A. (1996). "Application of Fracture Mechanics Principles to Analyze Cracking in Asphalt Concrete." Journal of the Association of Asphalt Paving Technologists, Vol. 65, pp. 1–39

8. Koohi, Y., Luo, R., Lytton, R. L., and Scullion, T. (2012). "New methodology to find the healing and fracture properties of asphalt mixes using overlay tester." Journal of Materials in Civil Engineering, ASCE, doi. 10. 1061/ (ASCE) MT.

9. Marasteanu, M. O., J. F. Labuz, S. Dai, and X. Li. (2002). "Determining the Low Temperature Fracture Toughness of Asphalt Mixtures." Transportation Research Record: Journal of the Transportation Research Board, No. 1789, pp. 191–199. Transportation Research Board of the National Academies, Washington, D.C.

10. Medani, T. O., and Molenaar, A. A. A. (2000). "Estimation of fatigue characteristics of asphalt mixes using simple tests." HERON, 45, (3), ISSN 0046-7316.

11. Pugno, N., Ciavarella, M., Cornetti, P. and Carpinteri, A. (2006). "A generalized Paris' law for fatigue crack growth." Journal of the Mechanics and Physics of Solids, 54, 1333–1349.

12. Roque, R., Birgisson, B., Sangpetngam, B., and Zhang, Z. (2002). "Hot mix asphalt fracture mechanics: A fundamental crack growth law for asphalt mixtures." 81st Annual Meeting of Transportation Research Board, CD-ROM, Washington D.C.

13. Wagoner, M. P., Buttlar, W. G., Paulino, G. H., and Blankenship, P. (2005). "Investigation of the fracture resistance of hot-mix asphalt concrete using a disk-shaped compact tension test." Transportation Research Record, Journal of the Transportation Research Board, No. 1929, 183–192, Transportation Research Board of the National Academies, Washington, D.C.

14. Walubita, L. F., A. N. M. Faruk, G. Das, H. A. Tanvir, J. Zhang, and T. Scullion (2012). "The Overlay Tester: A Sensitivity Study to Improve OT Repeatability and Minimize Variability in the OT Test Results". Research Report FHWA/TX-12/0-6607-1. Texas Transportation Institute, Texas A&M University System, College Station, Texas.

15. Walubita, L. F., Faruk, A. N. M., Alvarez, A. E., and Scullion, T. (2013). "The Overlay Tester (OT): using the fracture energy index concept to analyze the OT monotonic loading test data." Construction and Building Materials, 40, 802-811.

16. Zhang, Z., Roque, R., Birgisson, B., and Sangpetngam, B. (2001). "Identification and verification of a suitable crack growth law." 80th Annual Meeting of Transportation Research Board, CD-ROM, Washington D.C.

17. Zhou, F., S. Hu, T. Scullion, M. Mikhail, and L. F. Walubita. (2005). "A Balanced HMA Mix Design Procedure for Overlays." Journal of the Association of Asphalt Paving Technologists, Vol. 74, pp. 443-484.

18. Zhou, F., Hu, S., and Scullion, T. (2006). "Integrated asphalt (overlay) mixture design, balancing rutting and cracking requirements." FHWA/ TX-06/0-5123-1, Texas Transportation Institute, College Station, Texas.

19. Zhou, F., Hu, S., and Scullion, T. (2007). "Development and verification of the overlay tester based fatigue cracking prediction approach." FHWA/ TX-07/9-1502-01-8, Texas Transportation Institute, College Station, Texas.

20. Zhou, F., Hu S., and T. Scullion. (2009) "Overlay tester: a simple and rapid test for HMA fracture properties." Texas Transportation Institute, USA.

21. Zhou, F., and Scullion, T. (2003). "Upgraded overlay tester and its application to characterize reflection cracking resistance of asphalt mixtures" FHWA/ TX-04/0-4467-1, Texas Transportation Institute, College Station, Texas.

22. Zhou, F., and Scullion, T. (2005). "Overlay tester: a rapid performance related crack resistance test." FHWA/ TX-05/0-4467-2, Texas Transportation Institute, College Station, Texas.

23. Zhou, F. and T. Scullion, (2006). Overlay Tester: A Simple and Rapid Screening Test for Characterizing Crack Resistance of HMA Mixes, Proceedings of 10th International Conference on Asphalt Pavement, Quebec, Canada, August 12-17, 2006

Appendix A

Appendix A gives detailed information of the key variables associated with the Tex-248-F procedure that were thoroughly investigated.

GLUE TYPE

The current Tex-248-F test procedure calls for using a 2-part, 2-ton epoxy for gluing the specimens to the OT test plates. The suggested glue type acquires a maximum strength of 2500 psi when completely cured. To reduce the probability of failure of the OT specimens at the specimen-OT plate interface, it is critical to gain reliably a strong bond between the specimen and the OT plates. A glue with a higher strength was evaluated to compare its performance to the results obtained with the glue that is currently used.

While maintaining all other operational parameters the same, an additional glue with strength of 4400 psi was used. Monotonic load was applied to exert greater displacements than normally used in the OT tests. Figure A1 presents typical performances of the two (2500 psi and 4400 psi) glues under OT monotonic loading. The maximum load for the 4400-psi glue is slightly greater than that of the 2500-psi glue. The hysteresis loop obtained from the 4400-psi glue demonstrate a more linear behavior.

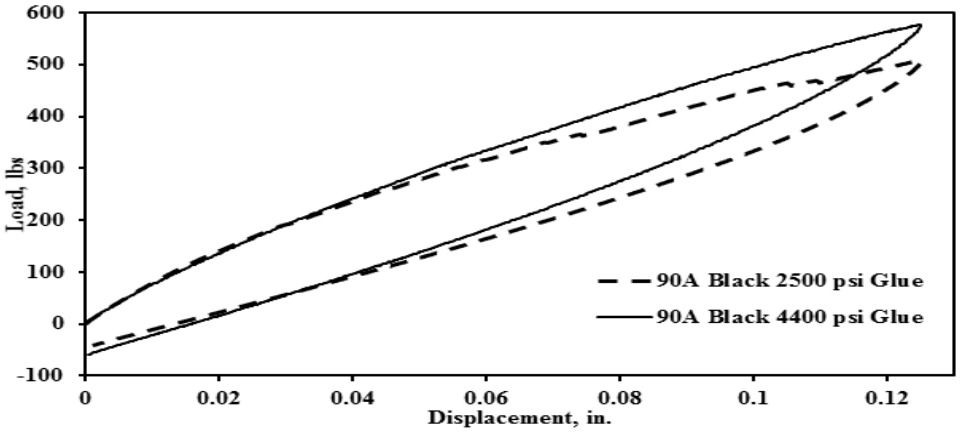

Figure A1: Comparison of Two Glue Types with Different Strength

GLUING METHOD

The last two versions of the OT specifications were studied to compare their gluing processes. The earlier version (called the "old" hereafter) Tex-248-F gluing method consisted of covering the gap between the base plates with adhesive tape to prevent the accumulation of glue. The adhesive tape and dry glue were removed with a hacksaw, after the glue hardened. By applying the old Tex-248-F gluing method, hardened glue may be encountered in the middle of the specimen. Even though the hardened glue is then removed with a hacksaw, the quality of the results may be operator-dependent.

The current Tex-248-F gluing method calls for pouring the glue on the large side of the trimmed specimen. Spacer bars are used to remove excess glue that accumulates between the OT plates after mounting the specimen. The new Tex-248-F specifies a more practical process of removing the accumulated glue when the glue is still fresh. Figure A2 illustrates typical load-deformation curves obtained from the new and old gluing methods. The maximum loads and the shapes of the hysteresis loops are different. This change in shape may be a consequence of the accumulated dry glue that was not removed with the hacksaw.

It was surmised that the repeatability of the OT tests will improve if the excess glue is removed from the trimmed specimen. The following items were further considered in order to improve the operational processes:

a) alternative method of using adhesive tape and spacer bars, and
b) alternative method of mixing and pouring of the glue.

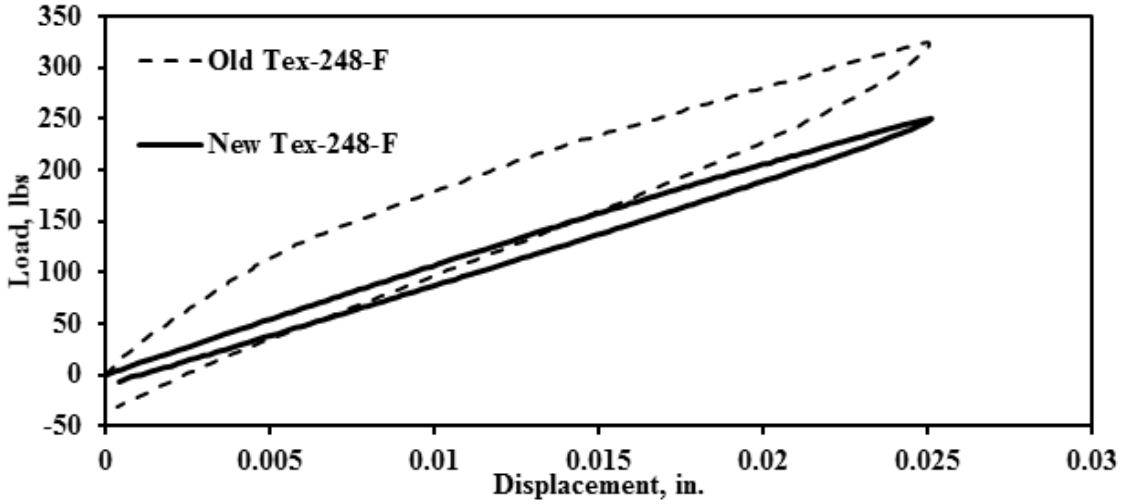

Figure A2: Comparison between Gluing Methods of Last Two Tex-248-F Versions

While maintaining all gluing variables constant, the synthetic specimens were tested with and without the application of tape. Petroleum jelly was applied between the tape and the specimen to facilitate the removal of the tape. As shown in Figure A3, the load-displacement response curves were somewhat different. The no-tape option resulted in a steeper slope, which can be caused by the accumulation of glue in the gap. The application of tape seems to be reasonable to improve the consistency of the glued area.

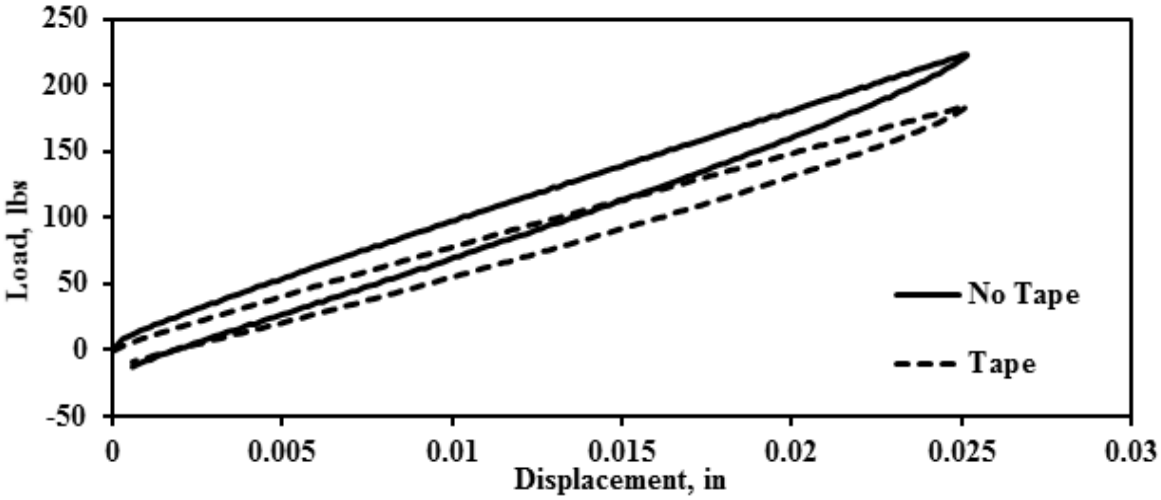

Figure A3 - Load-Displacement Response Curves with and without Tape

A consistent method to glue was considered essential. To that end, it was ensured that the glue was limited to the contact area between the OT specimen and the OT plates. To achieve this, the glue along the sides of the specimens was removed with a razor immediately after the glue was applied to the specimen. Figure A4 compares typical results obtained from the clean-sided specimens with normal gluing process included in Tex-248-F. For this task, only our medium (55D) synthetic specimen was tested. The specimens were subjected to monotonic loading until the glue failed. The two load-displacement curves are initially similar. One difference that was observed was the change in the slope of the specimen glued on the sides around 0.01 in. displacement. It was visually verified that the change in the slope could be attributed to the failure of the glue along the sides of the specimen. Also, the glue-on the-sides specimen failed at a greater displacement than the clean-sides specimens (0.04 in. as opposed to 0.02 in.).

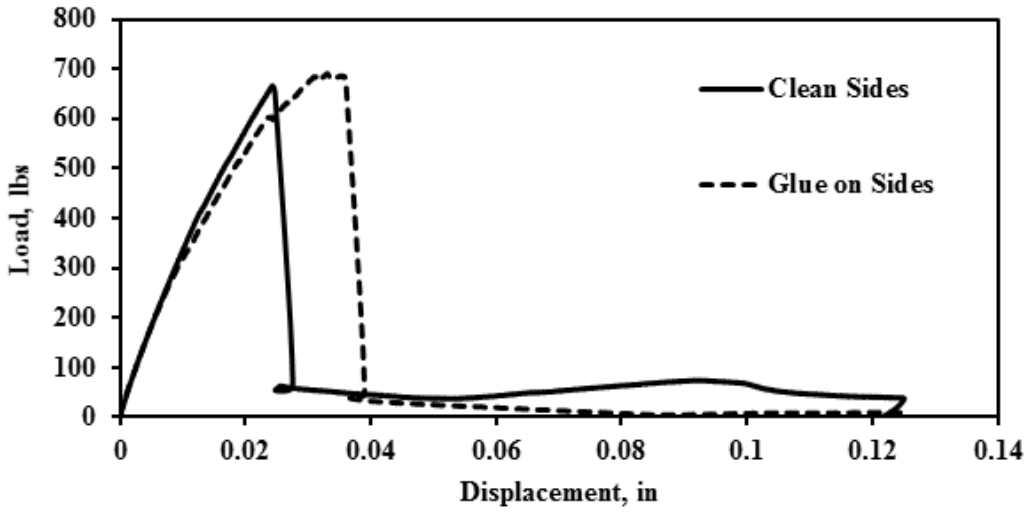

Figure A4: Clean Sides vs. Glue on Sides Load-Displacement Response Curves

In general, this comparison indicates that the glued area must be consistent to improve the repeatability in the results. Based on these preliminary results, a modified gluing method was designed to minimize the influence of the glued area.

MODIFIED GLUING METHOD

In addition to the gluing process proposed in the last (February 2014) version of Tex-248-F test protocol, the use of the tape and the removal of the glue located on the sides of the OT specimen are proposed for adoption in the future guidelines. The modified gluing process consists of the following steps:

1. Ensure the base plates and spacer bars are clean and free of any dirt or epoxy from the previous uses
2. Mount and secure the base plates to the mounting jig. Insert the spacer bar between the plates (apply a small amount of petroleum jelly on the spacer bar to facilitate its removal).
3. Draw a line along the middle of the trimmed specimen to guide the placement of the tape.
4. Place a piece of 4-mm-wide tape along the middle of the trimmed specimen to cover the gap (apply a small amount of petroleum jelly between the tape and the specimen to facilitate the tape removal once the specimen is mounted onto the base plates).
5. Prepare two containers containing 8 g of the two-part epoxy each. Prepare epoxy only for one specimen in one batch.
6. Evenly spread the glue in each container on one side of the trimmed specimen.
7. Glue the specimen to the base plates while ensuring that the specimen is centered and aligned with the edges of the base plates.
8. Add a 5-lb weight on top of the specimen to ensure intimate contact between the specimen and the base plates.
9. Remove the excess glue accumulated on the sides of the mounted specimen with a razor.
10. Remove the tape and then the spacer bar carefully to prevent the specimen from moving.

11. Allow the epoxy to cure for sufficient bonding strength as per manufacturer's recommendations (usually overnight is an adequate curing period).

Figure A5 illustrates the results obtained from the three different gluing methods (modified method, and new and Old Tex-248-F methods).

The load-displacement response curve from the modified methods was interpreted as a more consistent gluing method. To better understand the consistency of the modified gluing method, very soft (90A) synthetic specimen was tested three times. Figure A5 demonstrates the repeatability of the modified gluing method using a very soft (90A) synthetic specimen. The trends and maximum loads obtained from the three trials were similar. Thus, the modified gluing method is recommended for further evaluation.

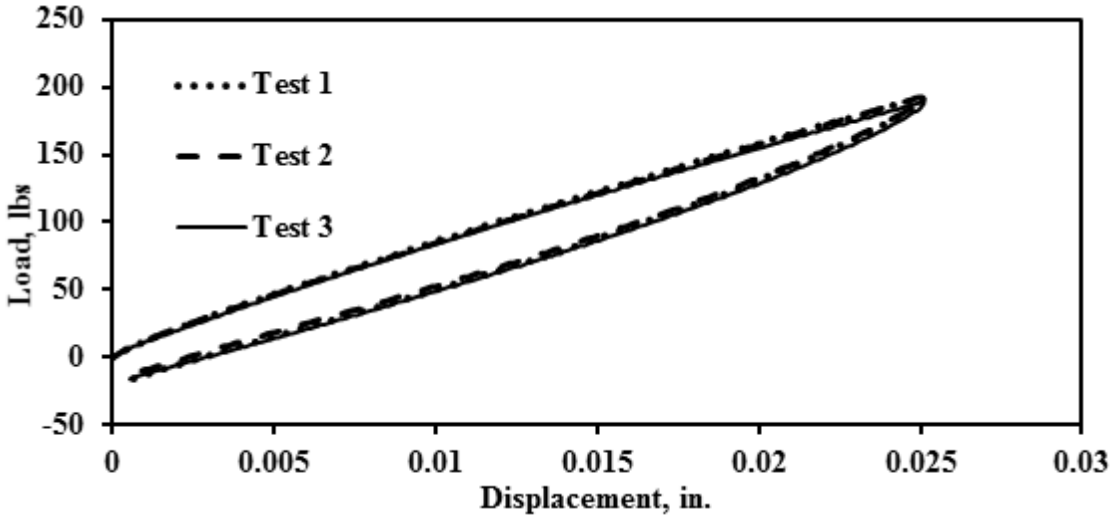

Figure A5: Consistency of Modified Gluing Method

Appendix B

Appendix B provides the correlation tables that were performed only for mix types which contained more than 3 sections. Type F, CAM, PFC, SP-C and SPD had from one to two sections each. Graphs are also presented on this Appendix showing the poor relationships found during this analysis.

Table B1: Type C Correlation Table (Sample Size 14 sections)

	Parameters	OT			OT-Fracture				
		Max. Load	No. of Cycles	Last Load	Max. Load	No. of Cycles	OT- E (Modulus)	*A*	*n*
IDT	Maximum Load	0.7	-0.9	0.3	0.2	-0.7	0.3	-0.7	0.4
	Displacement at Failure	-0.8	0.3	-0.8	0.0	0.3	0.0	0.3	-0.1
	Strength	0.7	-0.8	0.3	0.2	-0.7	0.3	-0.7	0.4
	Failure Strain	-0.8	0.3	-0.8	-0.5	0.0	-0.4	0.0	-0.3
	Modulus	0.7	-0.8	0.4	-0.1	0.7	-0.3	0.7	-0.4
OT-Fracture	Maximum Load	0.4	0.1	0.7					
	No. of Cycles	-0.3	0.4	-0.3					
	OT-E (Modulus)	0.4	0.1	0.7					
	A	-0.1	0.6	0.3					
	n	-0.2	0.1	-0.3					

Table B2: TOM Correlation Table (Sample Size 3 Sections)

	Parameters	OT			OT-Fracture				
		Max. Load	No. of Cycles	Last Load	Max. Load	No. of Cycles	OT- E (Modulus)	*A*	*n*
IDT	Maximum Load	1.0	1.0	0.8	1.0	0.6	1.0	-1.0	-1.0
	Displacement at Failure	1.0	1.0	0.8	1.0	0.6	1.0	-1.0	-1.0
	Strength	-1.0	-1.0	-0.8	-1.0	0.6	-1.0	1.0	1.0
	Failure Strain	1.0	1.0	0.8	1.0	0.6	1.0	-1.0	-1.0
	Modulus	0.5	0.5	0.9	0.5	0.6	0.5	-0.5	-0.5
OT-Fracture	Maximum Load	1.0	1.0	0.8					
	No. of Cycles	0.0	0.3	0.4					
	OT-E (Modulus)	1.0	1.0	0.8					
	A	-1.0	-1.0	-0.8					
	n	-1.0	-1.0	-0.8					

Table B3: SMA Correlation Table (Sample Size 4 Sections)

	Parameters	OT			OT-Fracture				
		Max. Load	No. of Cycles	Last Load	Max. Load	No. of Cycles	OT- E (Modulus)	*A*	*n*
IDT	Maximum Load	0.7	-0.5	0.7	-0.6	-0.1	0.4	-0.6	0.2
	Displacement at Failure	0.0	-0.7	-0.6	-0.5	-0.7	0.8	-0.4	-0.4
	Strength	0.7	0.1	1.0	-0.4	0.6	-0.3	-0.5	0.8
	Failure Strain	0.0	-0.7	-0.6	-0.5	-0.7	0.8	-0.4	-0.4
	Modulus	0.5	0.1	0.5	-0.3	0.8	-0.5	-0.4	0.9
OT-Fracture	Maximum Load	0.2	-0.9	-0.3					
	No. of Cycles	0.3	0.6	0.6					
	OT-E (Modulus)	0.2	-0.9	-0.3					
	A	-0.9	0.8	-0.5					
	n	0.7	0.1	0.8					

Table B4: CMHB-F Correlation Table (Sample Size 4)

	Parameters	OT			OT-Fracture			
		Max. Load	No. of Cycles	Last Load	Max. Load	OT- E (Modulus)	*A*	*n*
IDT	Maximum Load	1.0	1.0	1.0	0.9	0.9	0.5	-0.7
	Displacement at Failure	-1.0	-1.0	-1.0	-0.9	-0.9	-0.5	0.7
	Strength	1.0	1.0	1.0	0.9	0.9	0.5	-0.7
	Failure Strain	-1.0	-1.0	-1.0	-0.9	-0.9	-0.5	0.7
	Modulus	-0.3	-0.3	-0.4	-0.4	-0.4	-1.0	0.8
OT-Fracture	Maximum Load	0.9	0.9	0.9				
	OT-E (Modulus)	0.9	0.9	0.9				
	A	0.5	0.5	0.6				
	n	-0.7	-0.7	-0.8				

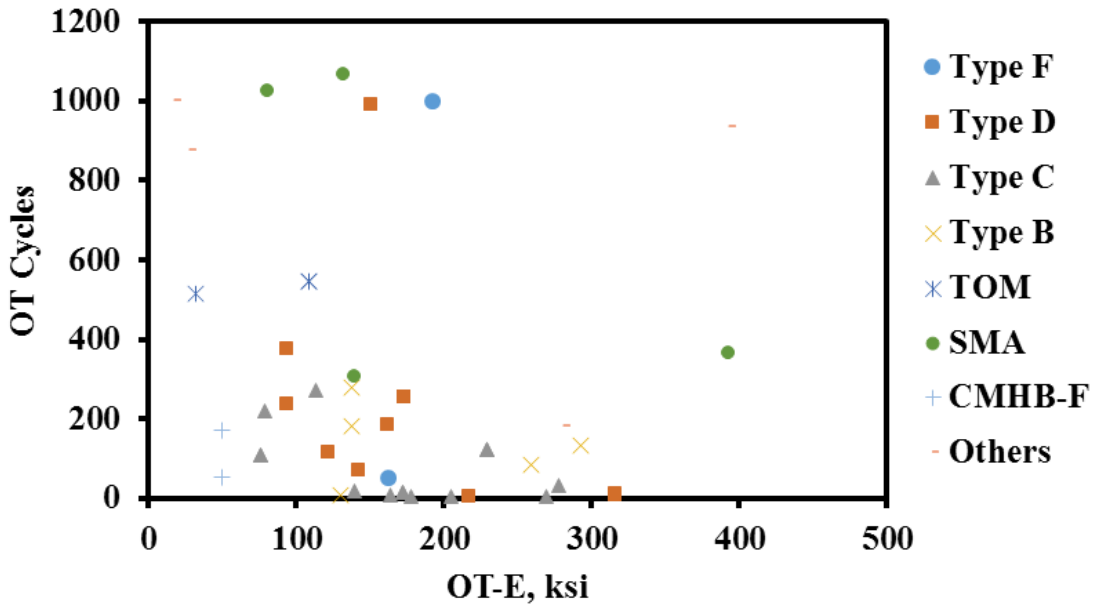

Figure B1: OT-E Compared with OT-Cycles

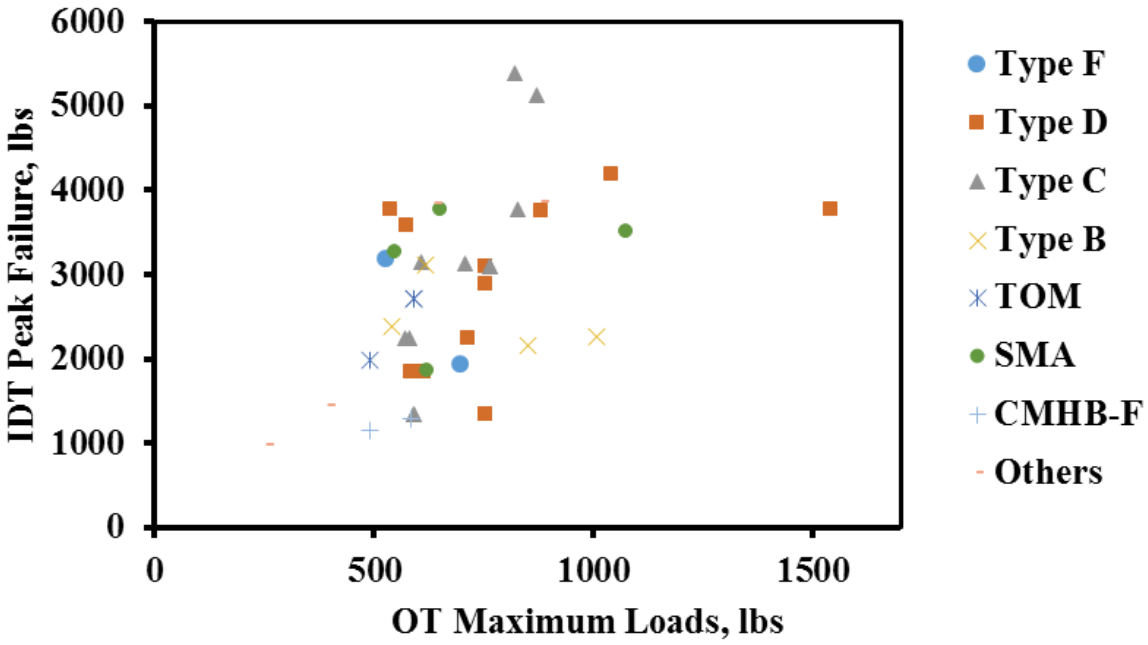

Figure B2: OT Maximum Loads Compared with IDT Peak Failure

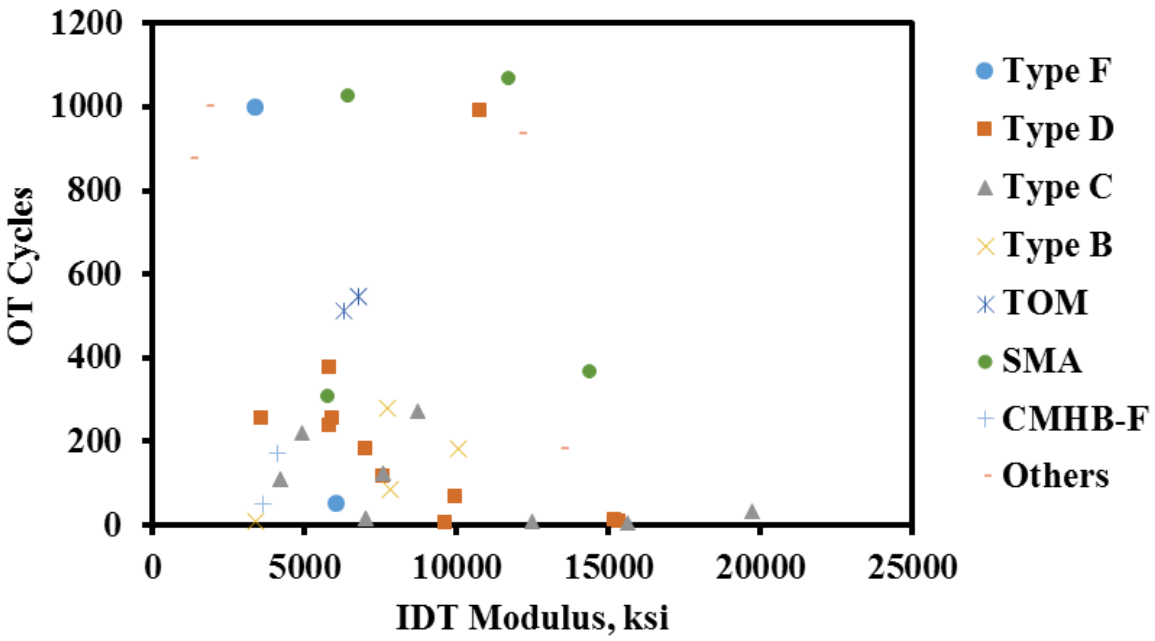

Figure B3: IDT Modulus compared with OT Cycles

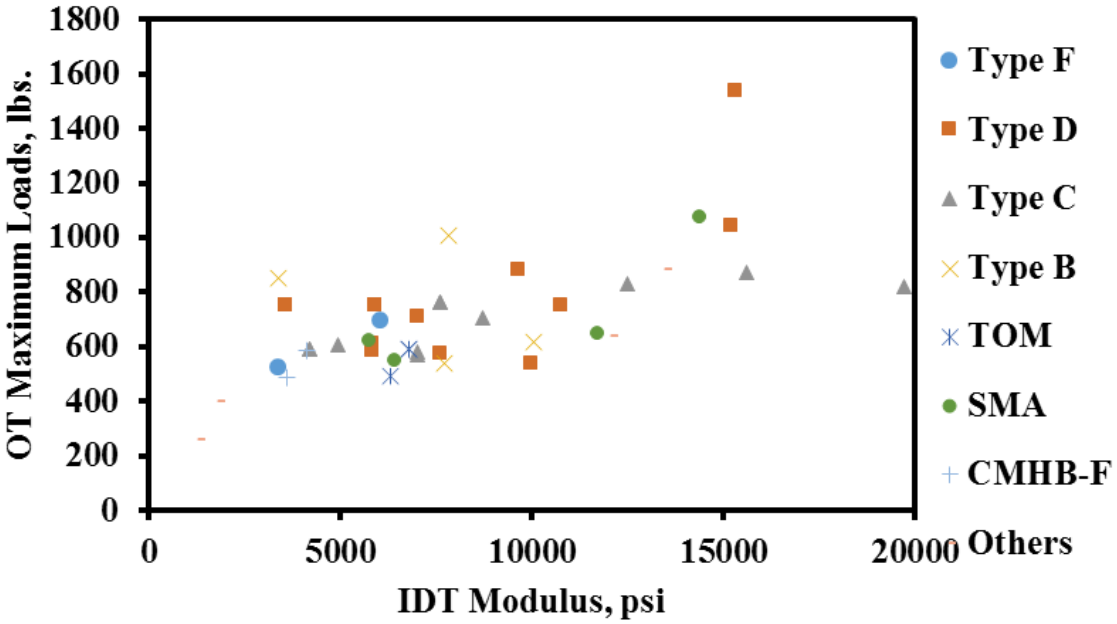

Figure B4: IDT Modulus Compared with OT Maximum Loads

Appendix C

Appendix C shows the median line of the total data of specimens of each mix. The error bars were also included on each median line. Finally, the trend line correspondent to different number of cycles to failure were also added on each graph.

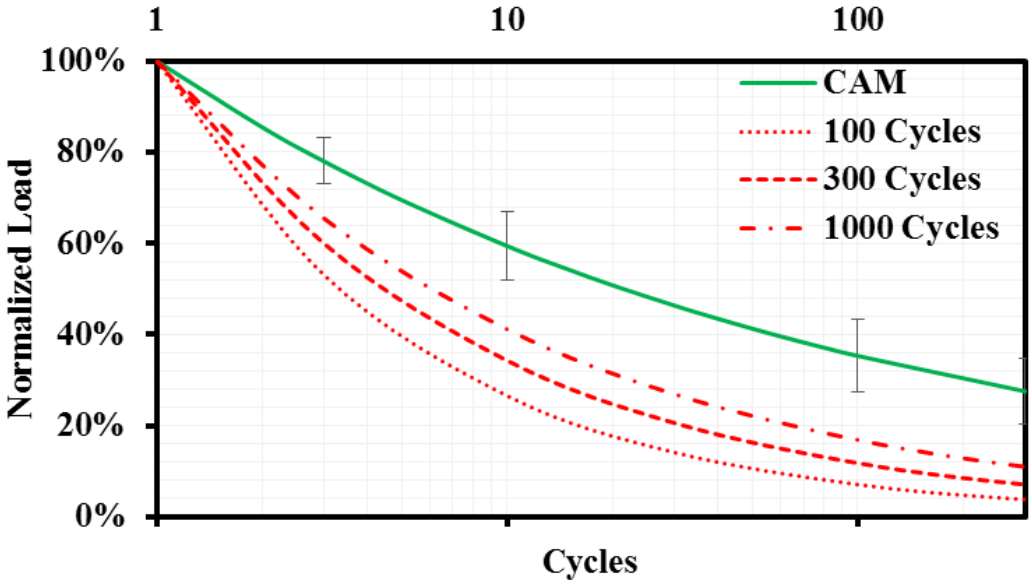

Figure C1: CAM Median Line

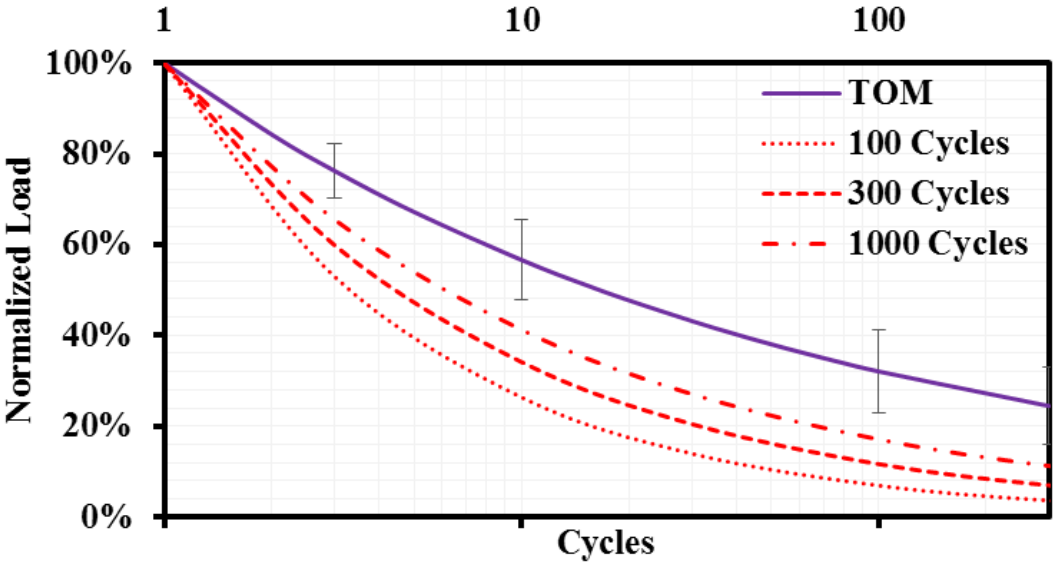

Figure C2: TOM Median Line

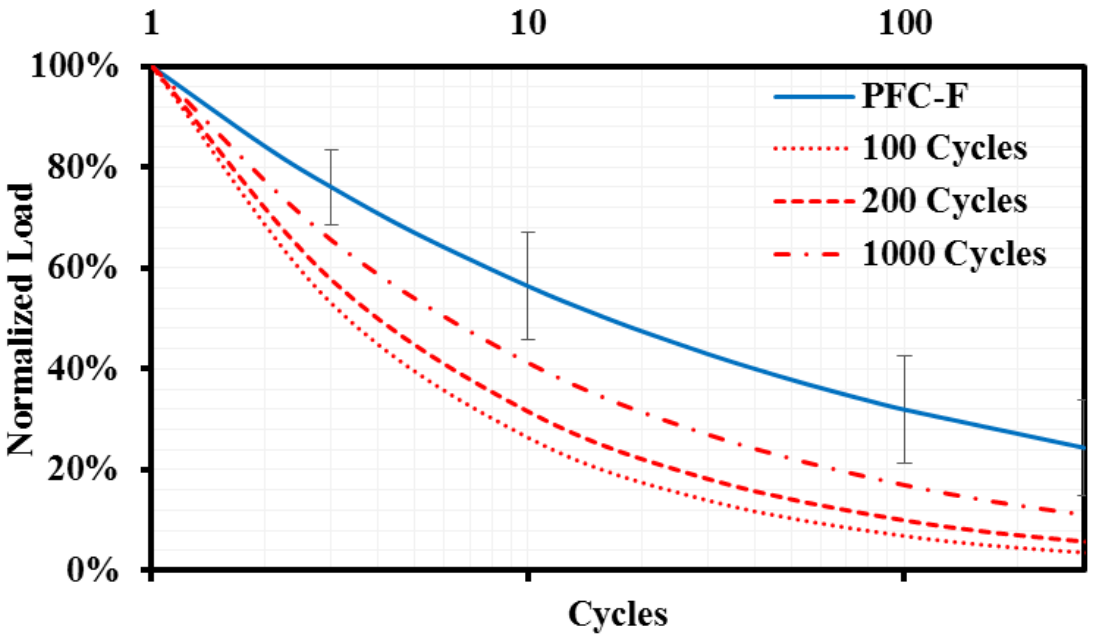

Figure C3: PFC-F Median Line

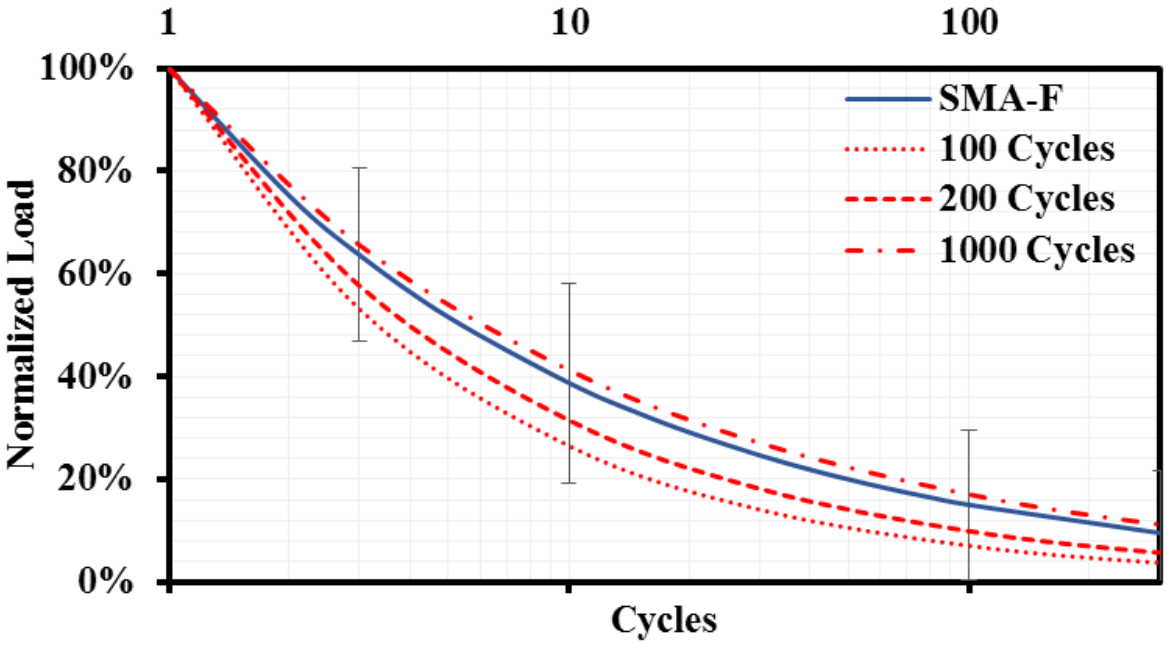

Figure C4: SMA-F Median Line

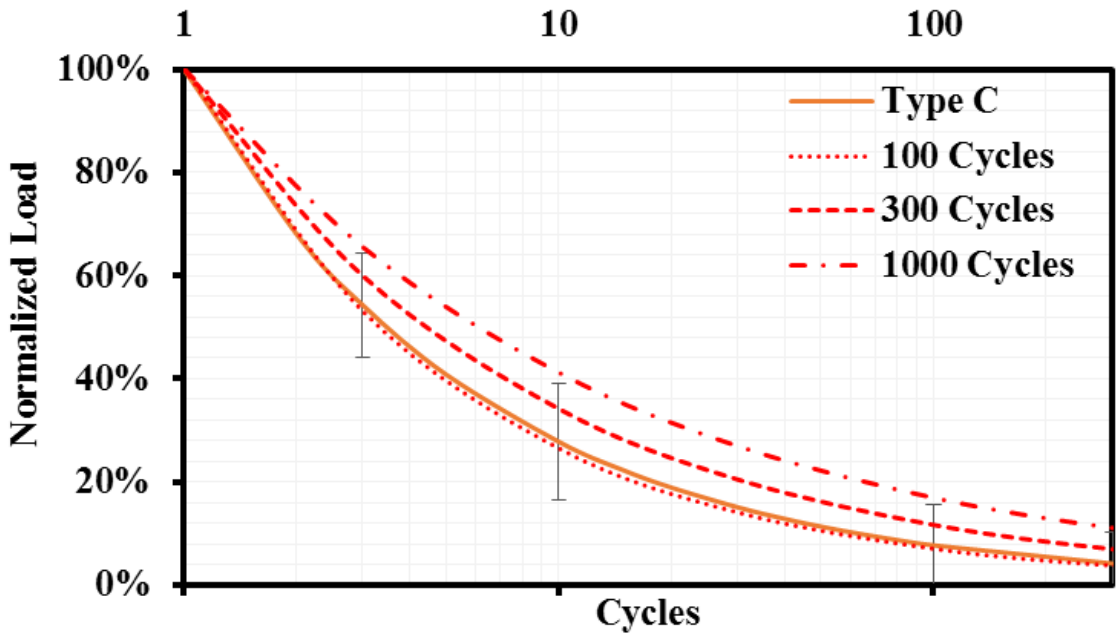

Figure C5: Type C Median Line

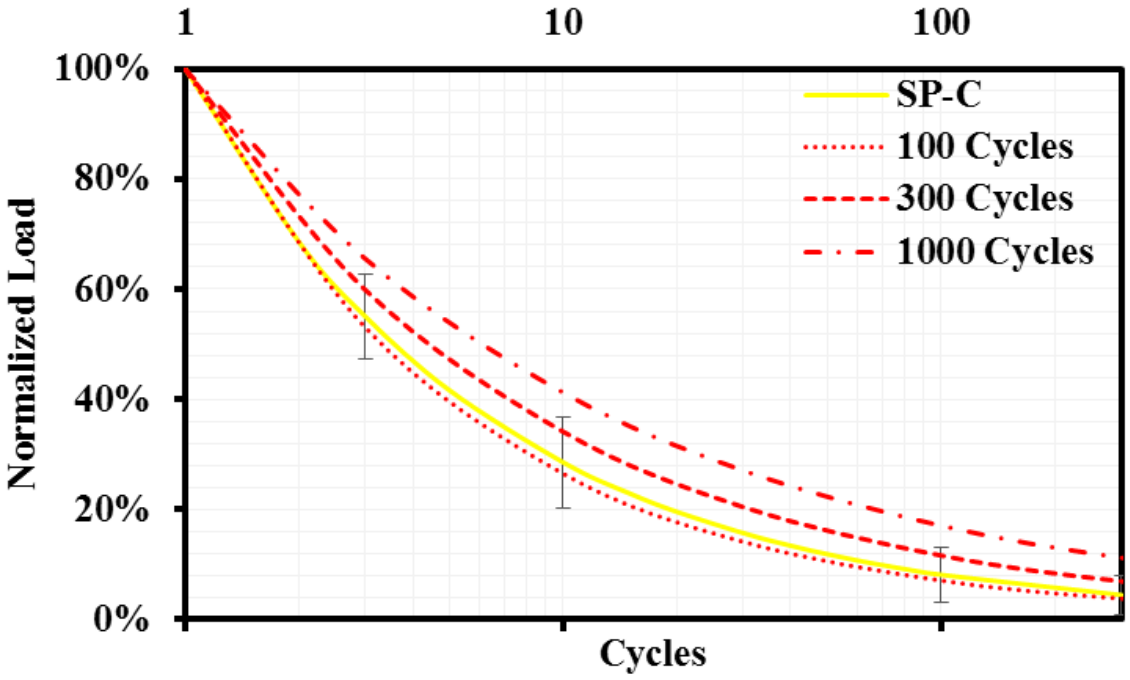

Figure C6: SP-C Median Line

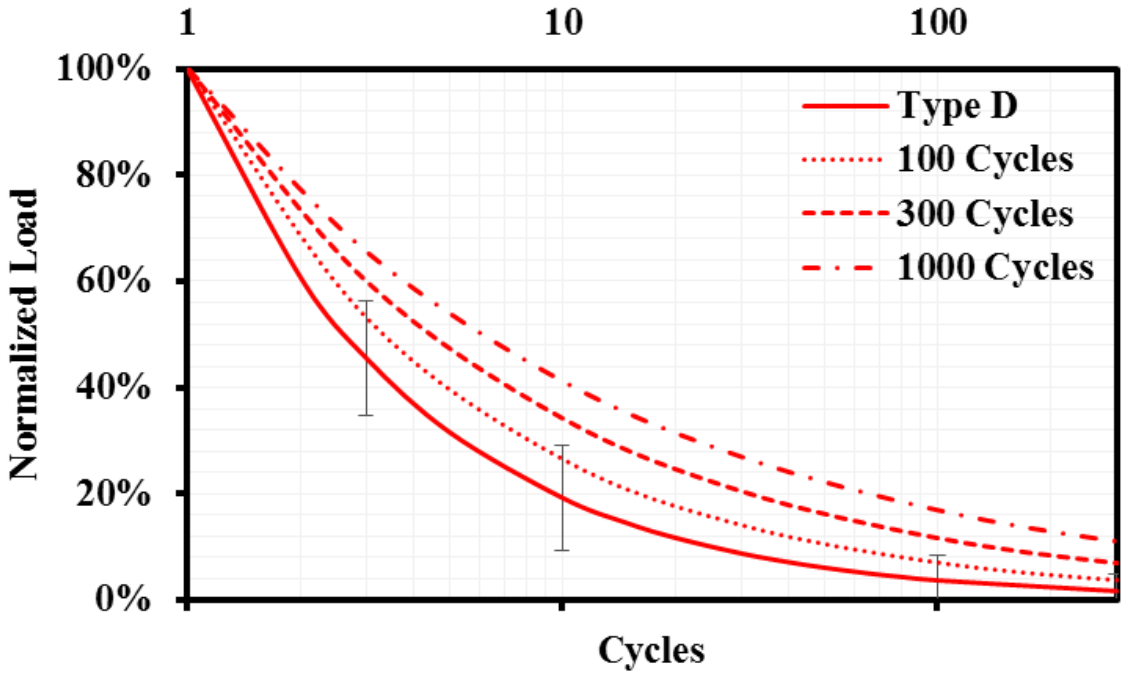

Figure C7: Type D Median Line

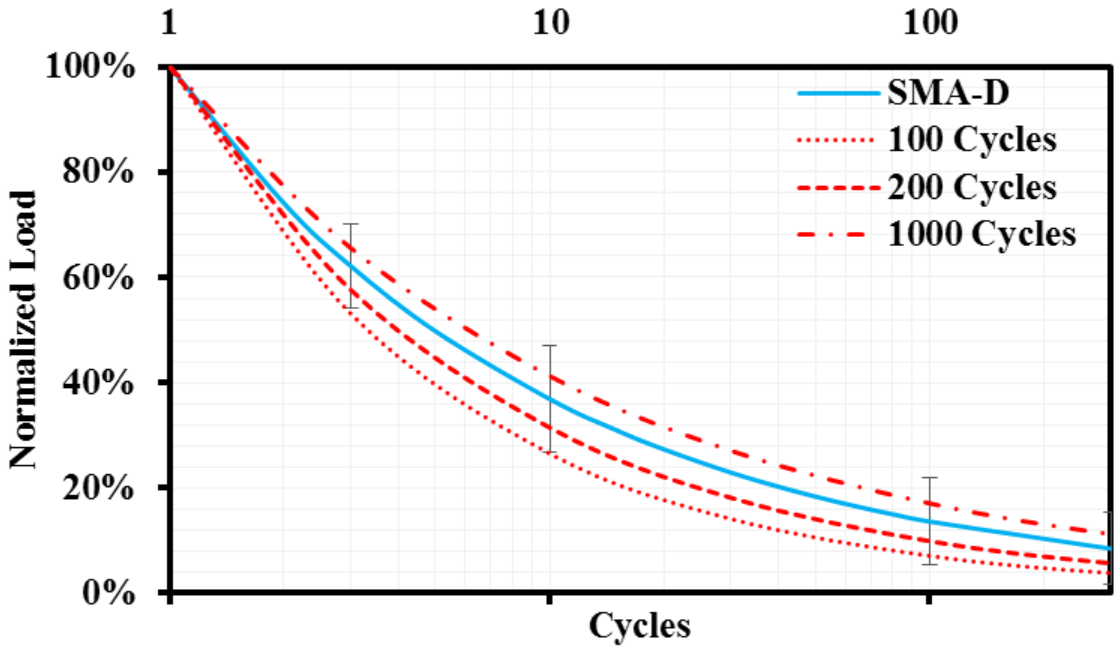

Figure C8: SMA-D Median Line

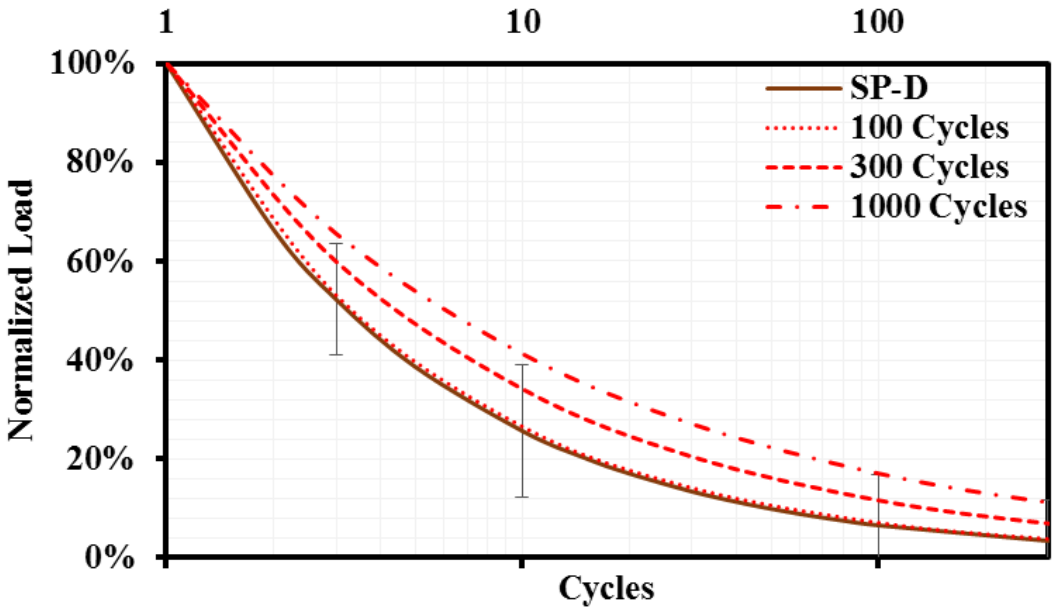

Figure C9: SP-D Median Line

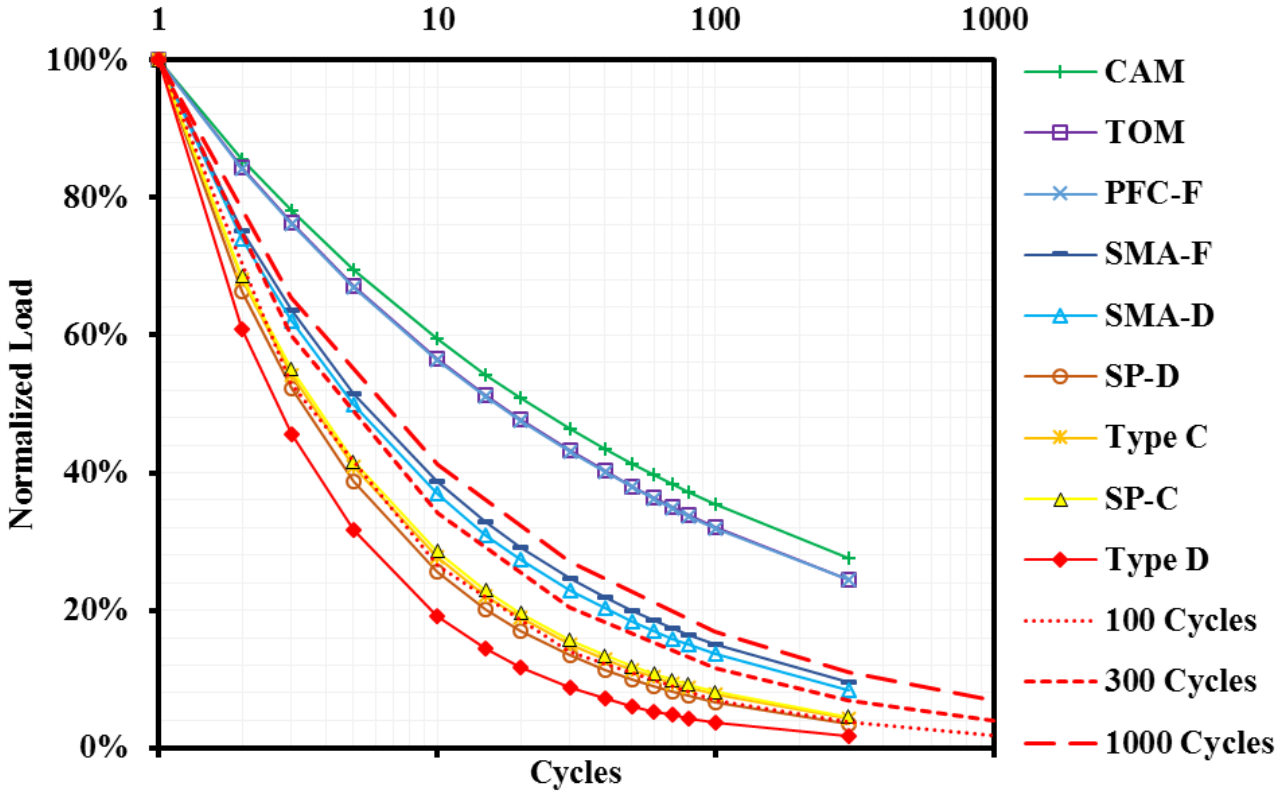

Figure C10: HMA mixes Delineation with Median Lines

Appendix D

Appendix D provides the cross plot graphs of load reduction versus fracture energy of each HMA mix. The black and red dotted lines represented the average and median load reduction rates, respectively. Data labels next to each dot represent the first cycle maximum load obtained from the OT test.

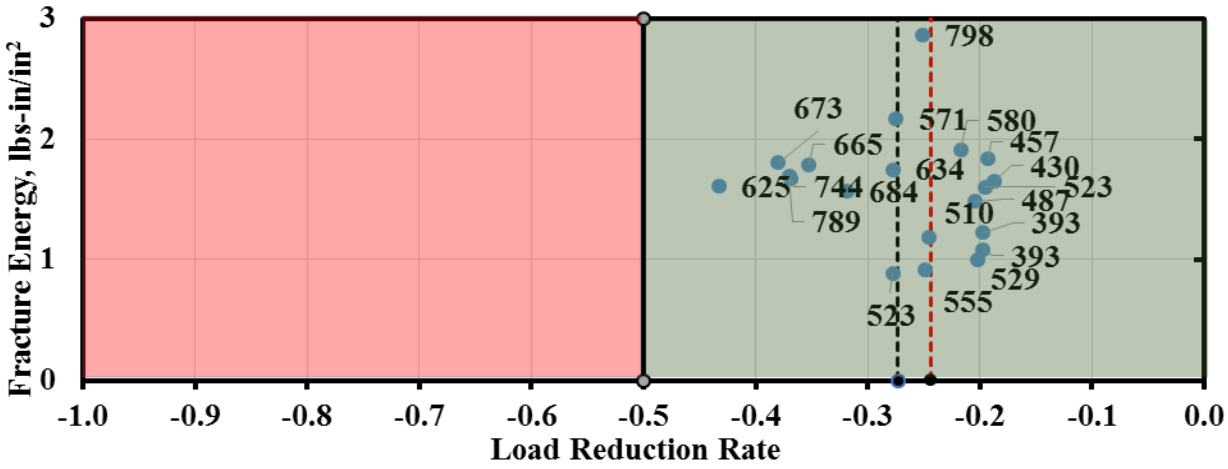

Figure D1: TOM Mix

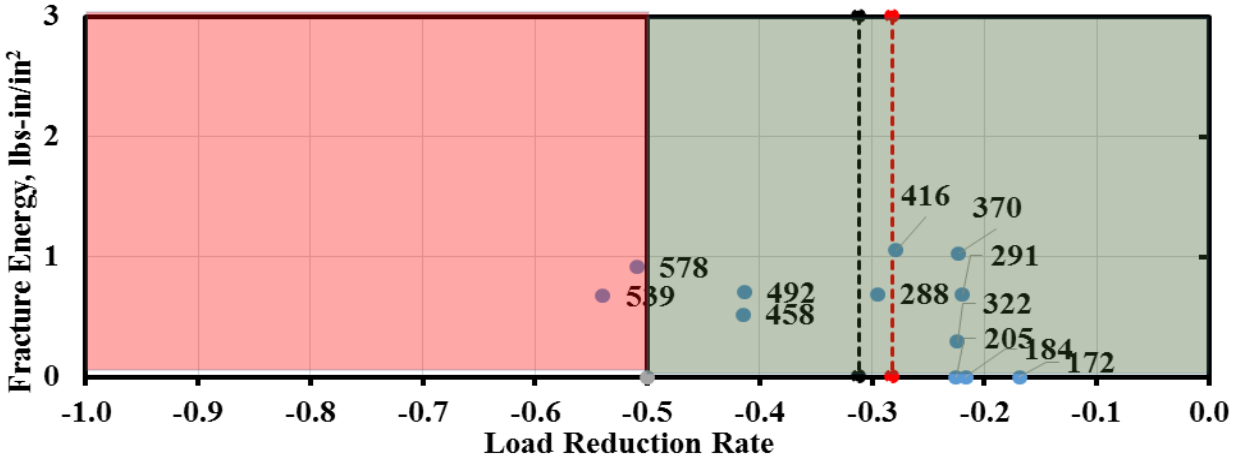

Figure D2: PFC-F Mix

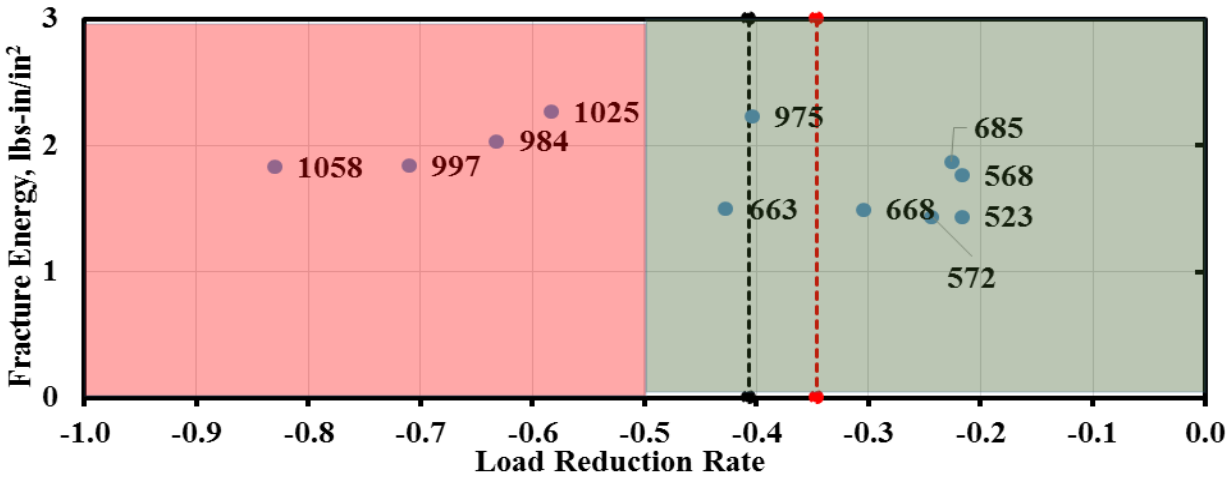

Figure D3: SMA-F

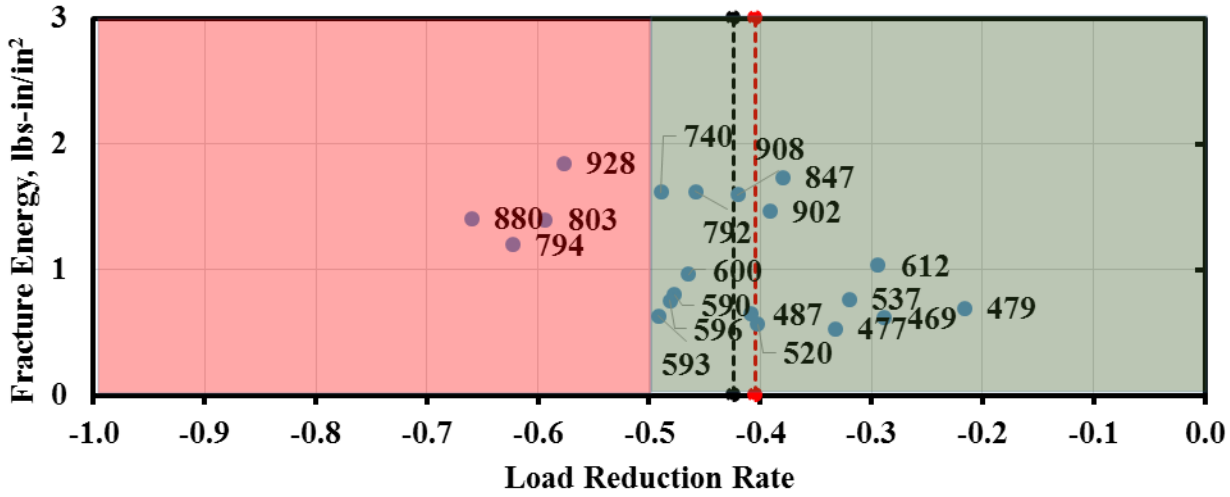

Figure D4: SMA-D Mix

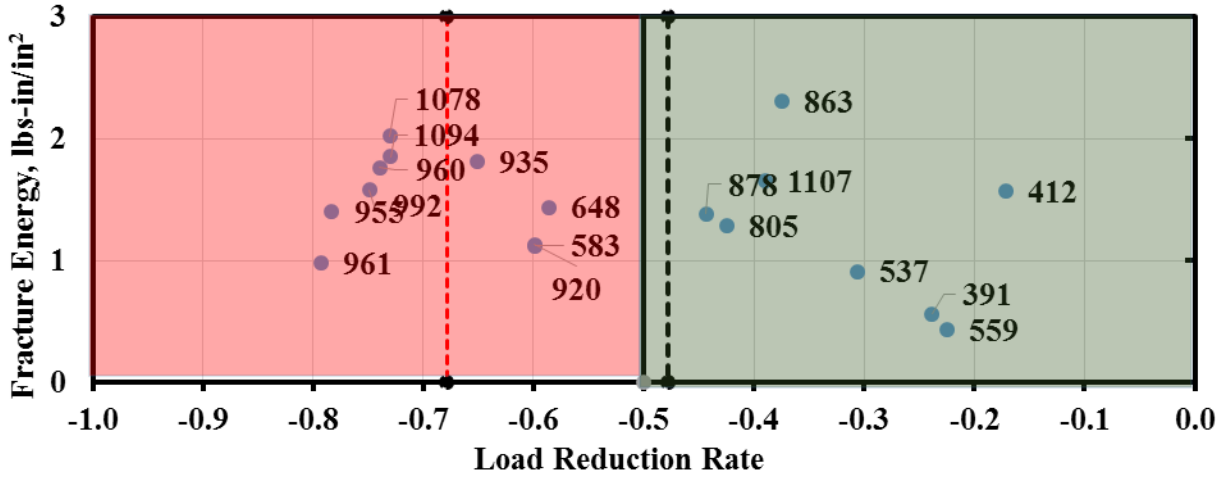

Figure D5: SP-D Mix

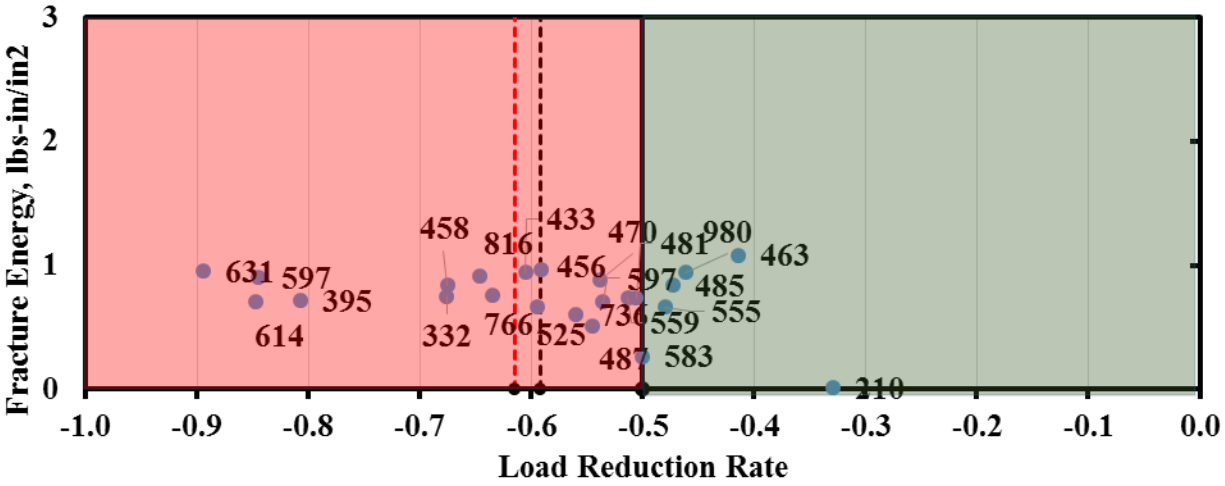

Figure D6: Type C Mix

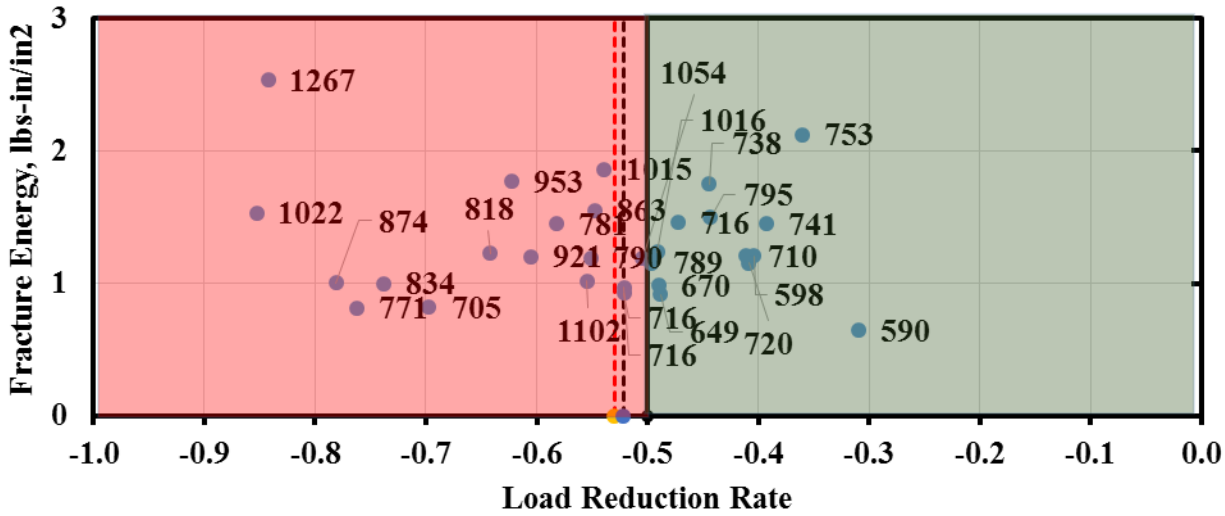

Figure D7: SP-C Mix

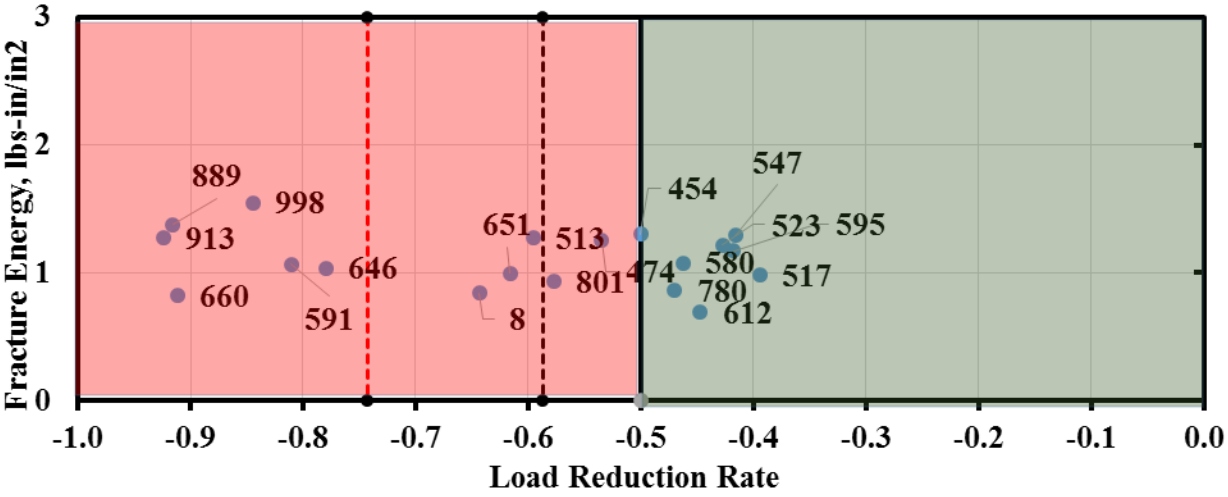

Figure D8: Type D Mix

Appendix E

Appendix E compares the repeatability of the current failure criteria (number of cycles to failure) with the implemented parameters. Each table shows the average of the set of triplicates, as well as the COV obtained.

Table E1: COV Results for CAM Mixes

CAM Sets	Load Reduction Rate		Fracture Energy,		Number of Cycles to Failure	
	Average	COV	Average, lbs-in./in.^{2}	COV	Average	COV
1	-0.483	4%	1.8	6%	1000	N/A
2	-0.247	4%	2.5	2%	1000	N/A
3	-0.220	4%	1.8	14%	454	25%
4	-0.237	5%	1.6	6%	1000	N/A
5	-0.465	18%	1.1	8%	1000	N/A
6	-0.389	6%	1.5	5%	1000	N/A
7	-0.189	1%	0.8	3%	1000	N/A
8	-0.722	4%	1.7	10%	245	38%
9	-0.441	8%	1.7	12%	646	19%
10	-0.213	6%	1.9	6%	377	83%
11	-0.443	20%	2.2	24%	441	81%
12	-0.216	5%	2.1	9%	50	22%

Table E2: COV Results for TOM Mixes

TOM Sets	Load Reduction Rate		Fracture Energy		Number of Cycles to Failure	
	Average	COV	Average, in.-lbs/in.^{2}	COV	Average	COV
1	-0.223	13%	1.2	26%	1000	N/A
2	-0.238	24%	1.0	14%	1000	N/A
3	-0.350	9%	1.7	8%	1000	N/A
4	-0.201	2%	1.4	13%	899	20%
5	-0.390	9%	1.7	3%	853	28%
6	-0.248	12%	2.2	28%	1001	N/A
7	-0.218	22%	1.9	14%	1001	N/A

Table E3: COV Results for PFC-F Mixes

PFC-F Sets	Load Reduction Rate		Fracture Energy		Number of Cycles to Failure	
	Average	COV	Average, in.-lbs/in.^{2}	COV	Average	COV
1	-0.300	32%	0.9	35%	262	49%
2	-0.241	18%	0.6	41%	1000	N/A
3	-0.463	11%	0.8	17%	1000	N/A

Table E4: COV Results for SMA-F Mixes

SMA-F Sets	Load Reduction Rate		Fracture Energy		Number of Cycles to Failure	
	Average	COV	Average, in.-lbs/in.^{2}	COV	Average	COV
1	-0.21	7%	1.5	12%	1000	N/A
2	-0.30	33%	1.6	13%	927	14%
3	-0.67	24%	1.5	47%	44	106%
4	-0.54	22%	2.1	11%	252	100%

Table E5: COV Results for SMA-D Mixes

SMA-D Sets	Load Reduction Rate		Fracture Energy		Number of Cycles to Failure	
	Average	COV	Average, in.-lbs/in.^{2}	COV	Average	COV
1	-0.46	19%	1.7	7%	538	78%
2	-0.42	11%	0.7	10%	254	38%
3	-0.33	17%	0.6	8%	256	97%
4	-0.52	13%	1.4	15%	256	97%
5	-0.32	38%	0.9	20%	856	29%
6	-0.46	24%	1.5	6%	426	92%
7	-0.41	21%	0.7	12%	519	81%

Table E6: COV Results for SP-D Mixes

SP-D Sets	Load Reduction Rate		Fracture Energy		Number of Cycles to Failure	
	Average	COV	Average, in.-lbs/in.^{2}	COV	Average	COV
1	-0.489	20%	1.3	10%	363	152%
2	-1.704	15%	1.5	1%	26	37%
3	-0.612	34%	2.1	11%	134	17%
4	-0.775	3%	1.3	23%	72	54%
5	-0.497	33%	1.2	23%	1000	N/A
6	-1.426	8%	1.4	38%	184	74%
7	-0.593	31%	1.7	5%	8	15%

Table E7: COV Results for SP-C Mixes

SP-C Sets	Load Reduction Rate		Fracture Energy		Number of Cycles to Failure	
	Average	COV	Average, in.-lbs/in.^{2}	COV	Average	COV
1	-0.453	30%	1.1	38%	9	42%
2	-0.490	9%	1.1	26%	210	31%
3	-0.388	10%	1.8	19%	590	40%
4	-0.329	5%	1.1	10%	6	9%
5	-0.523	6%	1.5	21%	102	21%
6	-0.631	6%	0.9	11%	19	38%
7	-0.426	6%	1.4	11%	445	31%
8	-0.523	10%	1.1	15%	88	18%
9	-0.424	11%	1.1	11%	561	69%
10	-0.652	12%	1.9	27%	44	67%
11	-0.557	16%	1.0	17%	61	76%

Table E8: COV Results for Type D Mixes

Type D Sets	Load Reduction Rate		Fracture Energy		Number of Cycles to Failure	
	Average	COV	Average, in.-lbs/in.^{2}	COV	Average	COV
1	-0.871	11%	1.5	6%	22	36%
2	-0.779	4%	0.9	24%	380	39%
3	-0.734	15%	1.3	14%	224	41%
4	-0.416	6%	1.2	9%	17	44%
5	-0.613	11%	1.0	3%	18	40%
6	-0.423	12%	1.2	14%	14	19%
7	-0.893	7%	1.9	6%	38	55%
8	-0.496	13%	1.1	31%	104	88%
9	-0.503	11%	0.9	5%	18	20%

Vita

Alejandro Miramontes was born in the United States, but pursued all his school in Mexico until his high school graduation in 2006. He attended The University of Texas at El Paso to pursue a Bachelors in Civil Engineering. During his senior year he started to work at the Center for Transportation Infrastructure Systems. Here he got involved in multiple research project working with asphalt binder and hot mix asphalt with the chance to perform several laboratory tests. Right after his bachelors' graduation, Alejandro decided to pursue a Master degree in the field of Geotechnical Engineering. During the beginning of his graduate studies, he presented a research project in the Transportation Research Board Conference in Washington DC with other fellow student. He co-authored a publication for this conference that was accepted for the yearly journal. He was involved in a research project sponsored by the Texas Department of Transportation.

Permanent address: 7518 Monterrey Dr.
El Paso, Texas, 79915

This thesis was typed by Alejandro Miramontes.